ortho C−H Activation of Haloarenes and Anisole by an Electron-Rich Iridium(I) Complex: Mechanism and Origin of Regio- and Chemoselectivity. An Experimental and Theoretical Study

Eyal Ben-Ari, Revital Cohen, Mark Gandelman, Linda J. W. Shimon, Jan M. L. Martin,* and David Milstein*

Department of Organic Chemistry, The Weizmann Institute of Science, 76100 Rehovot, Israel

Received January 24, 2006

Reaction of (PNP)Ir(COE)$^+PF_6^-$ (**1**) (PNP = 2,6-bis(di-*tert*-butylphosphinomethyl)pyridine; COE = cyclooctene) with benzene yields a stable unsaturated square pyramidal Ir(III) hydrido-aryl complex, **2**, which undergoes arene exchange upon reaction with other arenes at 50 °C. Upon reaction of **1** with haloarenes (chlorobenzene and bromobenzene) and anisole at 50 °C, selective *ortho* C−H activation takes place. No C−halogen bond activation was observed, even in the case of the normally reactive bromobenzene and despite the steric hindrance imposed by the halo substituent. The *ortho*-activated complexes (**8a**, **9a**, and **10a**) exhibited a higher barrier to arene exchange; that is, no exchange took place when heating at a temperature as high as 60 °C. These complexes were more stable, both thermodynamically and kinetically, than the corresponding *meta*- and *para*-isomers (**8b**,**c**, **9b**,**c**, and **10b**,**c**). The observed selectivity is a result of coordination of the heteroatom to the metal center, which kinetically directs the metal to the *ortho* C−H bond and stabilizes the resulting complex thermodynamically. Upon reaction of complex **1** with fluorobenzene under the same conditions, no such selectivity was observed, due to low coordination ability of the fluorine substituent. Competition experiments showed that the *ortho*-activated complexes **8a**, **9a**, and **10a** have similar kinetic stability, while thermodynamically the chloro and methoxy complexes **8a** and **10a** are more stable than the bromo complex **9a**. Computational studies, using the mPW1K exchange−correlation functional and a variety of basis sets for PNP-based systems, provide mechanistic insight. The rate-determining step for the overall C−H activation process of benzene is COE dissociation to form a reactive 14*e* complex. This is followed by formation of a η^2_{C-C} intermediate, which is converted into an η^2_{C-H} complex, both being important intermediates in the C−H activation process. In the case of chlorobenzene, bromobenzene, and anisole, η^1-coordination via the heteroatom to the 14*e* species followed by formation of the *ortho* η^2_{C-H} complex leads to selective activation. The unobserved C−halide activation process was shown computationally in the case of chlorobenzene to involve the same Cl-coordinated intermediate as in the C−H activation process, but it experiences a higher activation barrier. The *ortho* C−H activation product is also thermodynamically more stable than the C−Cl oxidative addition complex.

Introduction

The activation of strong C−H bonds of hydrocarbons is a topic of much current interest. Several examples of C−H bond activation under relatively mild conditions by transition metal complexes are known, and comprehensive mechanistic studies of this process have been reported.[1] Such studies are important for the design of efficient processes for the functionalization of hydrocarbons.

An attractive goal is the *selective* C−H bond activation of substituted arenes or alkanes. Murai *et al.* reported the regioselective catalytic *ortho*-hydroarylation of aromatic esters, ketones, and aldehydes based on metal coordination to the carbonyl group.[2−4] Amine, pyridyl,[5] hydroxy,[6] and/or other good coordinating groups have also been utilized. Recently, selective *ortho* C−H bond activation of acetophenone and nitrobenzene by an electron-rich (PCP)Ir complex was reported.[7,8] It was shown in this case that the selectivity is governed by thermodynamics rather than kinetics, i.e., stabilization of the C−H activation product by coordination of the *ortho* functional group to the metal, while coordination prior to C−H activation does not play a significant role.

* To whom correspondence should be addressed. E-mail: david.milstein@weizmann.ac.il; comartin@wicc.weizmann.ac.il.

(1) For reviews, see: (a) Lersch, M.; Tilset, M. *Chem. Rev.* **2005**, *105*, 2471. (b) Jones, W. D. *Inorg. Chem.* **2005**, *44*, 4475. (c) Labinger, J. A, Bercaw, J. E. *Nature* **2002**, *417*, 507. (d) Goldberg, K. I, Goldman, A. S., Eds. *Activation and Functionalization of C−H Bonds*; ACS Symposium Series 885; American Chemical Society: Washington, DC, 2004. (e) Jones W. D. *Acc. Chem. Res.* **2003**, *36*, 140. (f) Slugovc, C.; Padilla-Martinez, I.; Sirol, S.; Carmona, E. *Coord. Chem. Rev.* **2001**, *213*, 129. (g) Crabtree, R. H. *J. Chem. Soc., Dalton Trans.* **2001**, 2437. (h) Murai, S., Ed. *Topics in Organometallic Chemistry*, Vol. 3; Springer: New York, 1999. (i) Jensen, C. M. *Chem. Commun.* **1999**, *24*, 2443. (j) Shilov, A. E.; Shul'pin, G. B. *Chem. Rev.* **1997**, *97*, 2879. (k) Arndtsen, B. A.; Bergman, R. G.; Mobley, T. A.; Peterson, T. H. *Acc. Chem. Res.* **1995**, *28*, 154. (l) Jones, W. D.; Feher, F. J. *Acc. Chem. Res.* **1989**, *22*, 91 (m) Hill, C., Ed. *Activation and Functionalization of Alkanes*; John Wiley and Sons: New York, 1989. (n) Crabtree, R. H. *Chem. Rev.* **1985**, *85*, 245.

(2) Kakiuchi, F.; Matsumoto, M.; Sonoda, M.; Fukuyama, T.; Chatani, N.; Murai, S.; Furukawa, N.; Seki, Y. *Chem. Lett.* **2000**, 750.

(3) Kakiuchi, F.; Murai, S. *Acc. Chem. Res.* **2002**, *35*, 826, and references therein.

(4) (a) Kakiuchi, F.; Kan, S.; Igi, K.; Chatani, N.; Murai, S. *J. Am. Chem. Soc.* **2003**, *125*, 1698. (b) Asaumi, T.; Chatani, N.; Matsuo, T.; Kakiuchi, F.; Murai, S. *J. Org. Chem.* **2003,** *68*, 7538.

(5) Kakiuchi, F.; Igi, K.; Matsumoto, M.; Hayamizu, T.; Chatani, N.; Murai, S. *Chem. Lett.* **2002,** 396.

(6) Dorta, R.; Togni, A. *Chem. Commun.* **2003**, 760

(7) (a) Guari, Y.; Sabo-Etiennes, S; Chaudret, B. *J. Am. Chem. Soc.* **1998**, *120*, 4228. (b) Guari, Y.; Castellanos, A.; Sabo-Etiennes, S; Chaudret, B. *J. Mol. Catal. A* **2004,** *212*, 77.

(8) Zhang, X.: Kanzelberger, M.; Emge, J. T.; Goldman, A. S. *J. Am. Chem. Soc.* **2004**, *126*, 13192.

10.1021/om060078+ CCC: $33.50
Publication on Web 05/17/2006

Scheme 1

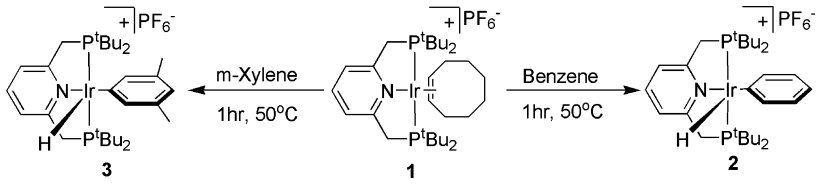

The chemo- and regioselective activation of strong C−H bonds in the presence of reactive substituents such as halides, is intriguing fundamentally and of potential synthetic importance. While there are a few reports of C−H bond activation of hydrocarbons in the presence of a C−Cl bond,[9−11] in most cases such chemoselectivity was demonstrated with systems in which C−Cl oxidative addition is difficult, such as late transition metal complexes of Ir and Rh having low electron density at the metal, or early transition metals, where the mechanism probably involves σ-bond metathesis. Moreover, coordination of halo-arenes to metal centers through the halide substituent is known to stabilize electron-poor, high-valent transition metal species.[12] Although examples of C−H activation of haloarenes by soluble late transition metal complexes were reported,[9,13,14] activation of the less hindered *meta* and *para* C−H bonds was observed due to steric reasons. Selective *ortho* C−H activation of fluoroarenes is known.[15,16] Recently, selective *ortho* C−H bond activation of chlorobenzene by a Zr complex was reported,[13] and competitive C−Cl and *ortho* C−H bond activation of chlorobenzene in the gas phase by FeO^+ is known.[9] We have reported an electron-rich, cationic PNP-type Ir(I) system that undergoes facile arene C−H bond activation, leading to *unsaturated, stable* arene−Ir(III) hydride complexes (Scheme 1).[17] This system exhibits chemo- and regioselectivity toward *ortho* C−H bond activation in chloro- and bromobenzene.[9] No C−halide oxidative addition was observed. The process was suggested to be directed by coordination of the metal to the halide substituent.

Here we report experimental and computational DFT studies that provide new insight into the C−H bond activation process and the reasons for the observed selectivity in the activation of chlorobenzene, bromobenzene, and anisole mediated by (PNP)-Ir(COE)$^+$PF$_6^-$ (**1**) (PNP = 2,6-bis(di-*tert*-butylphosphinomethyl)pyridine; COE = cyclooctene).

Scheme 2

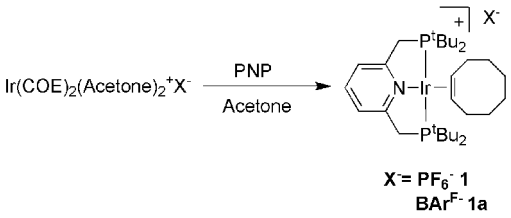

Experimental Results

Synthesis and Structure of the Complex (PNP)Ir(COE)$^+$, 1. The electron-rich, cationic, Ir(I) complex **1**[17] was prepared by addition of an equimolar amount of the PNP ligand (Scheme 2) to a yellow solution of the cationic complex [Ir(I)(acetone)$_2$-(COE)$_2$]$^+$PF$_6^-$ [18] in acetone, resulting in a color change to red-purple. ^{31}P{^{1}H} NMR revealed an AB quartet system at 46 ppm, indicative of a low-symmetry complex due to the sterically demanding environment around the metal center. Purple-red prismatic crystals of **1** were obtained by slow evaporation of its acetone solution. An X-ray crystallographic study revealed a distorted square planar geometry[19] (Figure 1, Table 1).

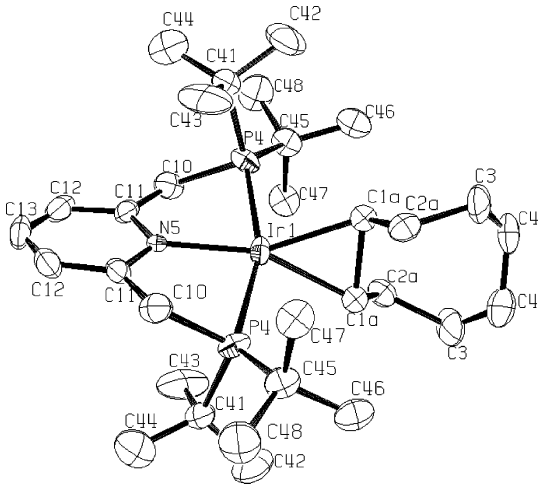

Figure 1. Structure of complex **1** (ORTEP drawing at 50% probability level; hydrogen atoms and the counteranion are omitted for clarity). For bond lengths and angles see Table 1.

Table 1. Selected Bond Lengths and Angles for 1

selected bond	bond length (Å)
Ir(1)−P(4)	2.3376(15)
Ir(1)−P(3)	2.3370(13)
Ir(1)−N(5)	2.103(5)
selected bond	**bond angle (deg)**
N(5)−Ir(1)−P(4)	79.84(4)
N(5)−Ir(1)−P(3)	90.2(4)
C(1)−Ir(1)−P(3)	85.6(3)
C(2)−Ir(1)−P(3)	94.3(4)
C(1)−Ir(1)−P(4)	94.4(4)
C(2)−Ir(1)−P(4)	85.5(6)

Reaction of [Ir(COE)$_2$Cl]$_2$ with sodium tetrakis[3,5-bis(trifluoromethyl)phenyl]borate (NaBAr^F) in acetone followed by ad-

(9) Competitive *ortho* C−H and C−Cl bond activation of chlorobenzene by FeO^+ in the gas phase: Bronstrup, M.; Trage, C.; Schröder, D.; Schwartz, H. *J. Am. Chem. Soc*. **2000**, *122*, 699.

(10) Vetter, A. J.; Jones, W. D. *Polyhedron* **2004**, *23*, 413.

(11) (a) Arndtsen, B. A.; Bergman, R. G. *Science* **1995,** *270*, 1970. (b) Tellers, D. T.; Yung, C. M.; Arndtsen, B. A.; Adamson, D. R.; Bergman, R. G. *J. Am. Chem. Soc.* **2002,** *124*, 1400. (c) Y. Fuchita, Y. Utsunomiya, M. Yasutake, J. *Chem. Soc. Dalton Trans.* **2001**, 2330. (d) Fan, L.; Parkin, S.; Ozerov, O. V. *J. Am. Chem. Soc.* **2005**, *127*, 16772.

(12) (a) Crabtree, R. H.; Faller, J. W.; Mellea, M. F.; Quirk, J. M.; *Organometallics* **1982**, *1*, 1361. (b) Burk, M. J.; Crabtree, R. H. *J. Organomet. Chem* **1988**, *341*, 495. (c) Kulawiec, R. J.; Crabtree, R. H.; *Coord. Chem. Rev.* **1990**, *99*, 89.

(13) Wu, F.; Dash, A. K.; Jordan, R. F. *J. Am. Chem. Soc.* **2004**, *126*, 15360.

(14) (a) Cho, J. Y.; Tse, M. K.; Holmes, D.; Maleczka, R. E., Jr.; Smith, M. R., III. *Science* **2002**, *295*, 305. (b) Ishiyama, T.; Takagi, J.; Ishida, K.; Miyaura, N.; Anastasi, N. R.; Hartwig, J. F. *J. Am. Chem. Soc.* **2002**, *124*, 390.

(15) (a) Clot, E.; Oelckers, B.; Hugo, A. K.; Eisenstein, O.; Perutz, R. N. *Dalton Trans.* **2003**, 4065. (b) Renkema, K. B.; Bosque, R.; Streib, W.; Maseras, F.; Eisenstein, O.; Caulton, K. G. *J. Am. Chem. Soc.* **1999**, *121*, 10895.

(16) Selmeczy, D. A.; Jones, D. W.; Partridge, G. M.; Perutz, R. N. *Organometallics*, **1994**, *13*, 522.

Scheme 3

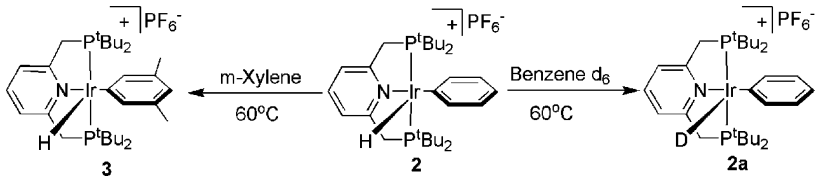

Scheme 4

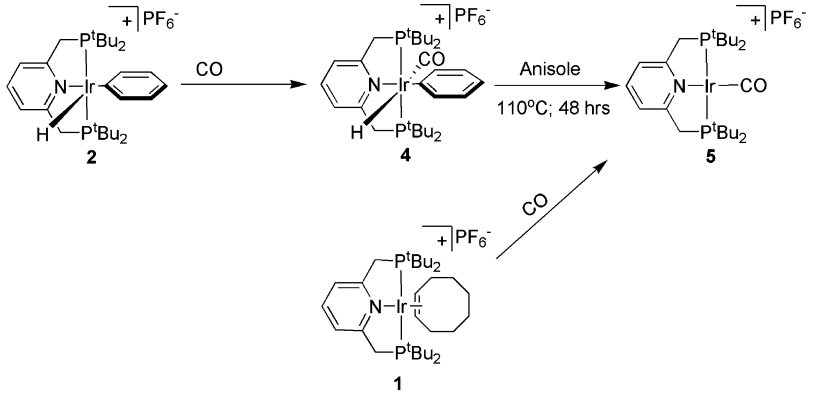

dition of 2 equiv of the PNP ligand resulted in formation of complex (PNP)Ir(COE)$^+$BAr^{F-} in 80% yield (Scheme 2).

The unique reactivities of these complexes toward C−H activation of benzene, haloarenes, and anisole were investigated experimentally and theoretically. Both complex **1** and complex **1a** were studied, and the same reactivity was observed.

Reaction of (PNP)Ir(COE)$^+$ with Benzene. Heating of complex **1** at 50 °C for 1 h (or at 25 °C for 48 h) in benzene resulted in formation of the unsaturated aryl hydride complex **2** (Scheme 1). ^{31}P NMR of this complex revealed a doublet at 54 ppm with $^2J_{HP}$ = 13 Hz, characteristic of *cis* hydrogen−phosphorus coupling. ^{1}H NMR exhibited a triplet at −44 ppm, indicative of a hydride located *trans* to a vacant coordination site. Orange prismatic crystals were obtained by slow evaporation of a benzene solution of **2**. Single-crystal X-ray analysis revealed a slightly distorted square pyramidal geometry around the metal center, the hydride being located at the axial site.[17]

Although complex **2** is coordinatively unsaturated, it exhibited high stability, showing no decomposition upon heating as a solid at 100 °C for 24 h. However, when heated at 60 °C in *m*-xylene, arene exchange took place, resulting in the *m*-xylyl complex **3** (Scheme 3), which was synthesized independently by heating **1** in *m*-xylene at 50 °C (Scheme 1). Furthermore, when complex **2** was heated at 60 °C in C_6D_6, disappearance of the hydride ligand and appearance of a deuteride were observed, indicating formation of (PNP)Ir(D)(C_6D_5), **2a** (Scheme 3).

Complex **2** represents a rare example of a thermally stable coordinatively unsaturated M(III) d^6 hydrido-aryl complex. Such species are proposed as reactive intermediates in several transition metal-catalyzed processes.[3,6,20] Werner reported the only example of a crystallographically characterized, thermally stable, unsaturated Ir(H)(R) (R = aryl, alkyl) complex, Ir(P^{i}Pr$_3$)$_2$(H)(C_6H_5)(Cl).[21] Recently, Goldman reported a closely related unsaturated complex, (PCP)Ir(H)(C_6H_5) (PCP = 2,6-(tBu_2PCH_2)$_2C_6H_3$).[22] This thermally unstable complex was characterized in solution and exhibited fast arene exchange even at low temperature, which followed a dissociative mechanism.[22] Intuitively, it seems that the main difference between these isoelectronic systems is the electron density at the iridium centers. Since a lower electron density is expected at the iridium center of the cationic (PNP)Ir system, that should result in more facile reductive elimination and lower thermal stability, the observed higher stability of the PNP system is surprising. It could be argued that a reductive addition process[23] took place, increasing the electron density on the (PNP)Ir system after addition of the C−H bond. To address the question of relative electron density on the cationic Ir(I) and Ir(III) PNP-based systems (and to compare it to the relevant PCP-based neutral Ir complex), the corresponding carbonyl complexes were prepared. Addition of 1 equiv of CO to a DMSO solution of (PNP)Ir(H)(C_6H_5) (**2**) resulted in formation of (PNP)Ir(H)(C_6H_5)(CO) (**4**) (Scheme 4).

The ^{31}P{^{1}H} NMR spectrum of **4** revealed a signal at 45 ppm, and ^{1}H NMR exhibited the hydride ligand as a triplet at −7.5 ppm, representing a large downfield shift compared to the corresponding hydride signal of complex **2** (−44 ppm). Such a shift indicates coordination of the CO *trans* to the hydride ligand. In addition, ^{13}C{^{1}H} NMR revealed a characteristic signal at 183 ppm for the Ir−CO bond.

A comparison of the CO absorption frequency of (PCP)Ir(CO)(H)(C_6H_5)[22] (1973 cm^{-1}) with that of (PNP)Ir(H)(C_6H_5)(CO) (**4**) (2005 cm^{-1}) indicates that the electron density at the cationic Ir(III) center in **4** is lower, as expected. Moreover, the CO stretching frequencies of (PNP)Ir(CO) **5** (1964 cm^{-1}) and **4** (2005 cm^{-1}) indicate a significantly lower electron density on the Ir(III) center of **4**. This indicates that C−H oxidative addition rather then reductive addition took place. Complex **5**

(17) Ben-Ari, E.; Gandelman, M.; Rozenberg, H.; Shimon, L. J. W.; Milstein, D. *J. Am. Chem. Soc.* **2003**, *125*, 4714.

(18) Preparation of this complex in solution was reported: Bosch, M.; Werner, H. *Eur. J. Inorg. Chem.* **2001**, 3181. Recently we isolated it as a yellow solid: Dorta, R.; Rozenberg, H.; Shimon, L. J. W.; Milstein, D. *J. Am. Chem. Soc*. **2002**, *124*, 188.

(19) Due to disorder of the cyclooctene ligand, it was impossible to determine its bond lengths.

(20) (a) Doughty, D. H.; Pignolet, L. H. *J. Am. Chem. Soc*. **1978**, *100*, 7083.

(21) Werner, H.; Höhn, A.; Dziallas, M. *Angew. Chem., Int. Ed. Engl.* **1986**, *12*, 1090.

(22) Kanzelberger, M.; Singh, B.; Czerw, M.; Krogh-Jespersen, K.; Goldman, A. S. *J. Am. Chem. Soc.* **2000**, *122*, 11017.

(23) Crabtree, R. H.; Quirk, J. M. *J. Organomet. Chem.* **1980**, *199*, 99.

Scheme 5

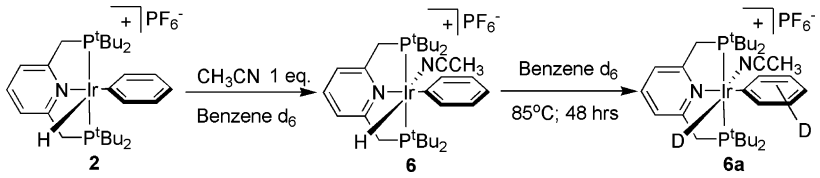

was prepared by the facile reaction of complex **1** with 1 equiv of CO (Scheme 4).

Interestingly, elimination of benzene from complex **4** occurred only when it was heated to a temperature as high as 110 °C for 48 h, resulting in quantitative formation of (PNP)Ir(CO), **5** (Scheme 4). The octahedral (PNP)Ir(H)(C_6H_5)(CO) complex, **4**, like Goldman's (PCP)Ir(H)(C_6H_5)(CO) complex, is kinetically stabilized toward reductive elimination of benzene, which is expected to involve ligand loss.[24] Complex **5** did not exhibit C−H oxidative addition reactivity, as no reaction took place when it was heated in anisole at 110 °C. Noteworthy, addition of acetonitrile to complex **2** resulted in the formation of complex **6**, which was crystallographically characterized, exhibiting an octahedral structure with the nitrile ligand coordinated *trans* to the hydride ligand in an end-on fashion (Figure 2, Table 2). A comparison of the C−N triple bond length of free acetonitrile (1.158 Å)[25] with the C(2)−N(1) bond length of 1.134 Å indicates that there is very little back-donation from the metal to the nitrile group.

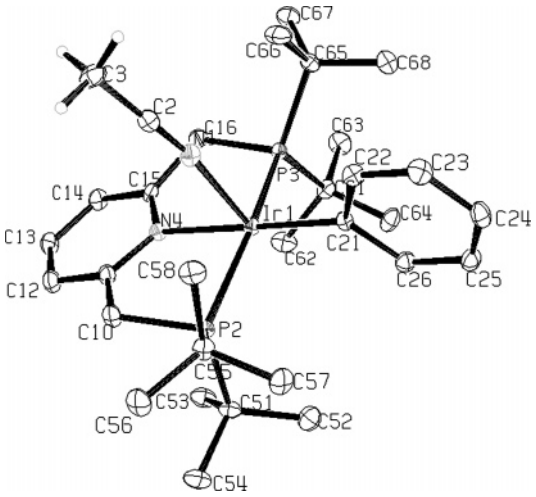

Figure 2. Structure of **6** (ORTEP drawing at 50% probability level; hydrogen atoms and counteranion are omitted for clarity). For selected bond lengths and angles see Table 2.

Table 2. Selected Bond Lengths and Angles for 6

selected bond	bond length (Å)
Ir(1)−C(21)	2.072(2)
Ir(1)−P(3)	2.3291(9)
Ir(1)−P(2)	2.3304(9)
Ir(1)−N(1)	2.153(2)
Ir(1)−N(4)	2.157(2)
C(2)−N(1)	1.134(1)
C(2)−C(3)	1.46(2)
selected bond	**bond angle (deg)**
N(1)−Ir(1)−P(3)	97.78(6)
N(1)−Ir(1)−C(21)	95.83(3)
N(4)−Ir(1)−C(21)	178.11(8)
N(4)−Ir(1)−N(1)	82.44(9)
N(1)−C(2)−C(3)	178.5(3)
C(21)−Ir(1)−P(3)	98.25(7)

Complex **6** does not eliminate benzene upon heating in C_6D_6 even at 70 °C. However, at higher temperature it exhibits arene exchange (Scheme 5).

The kinetic isotope effect of the C−H activation process of benzene was determined by dissolving (PNP)Ir(COE)$^+PF_6^-$ (**1**) in a 1:1 molar ratio of C_6H_6:C_6D_6 and leaving the solution at 25 °C for 48 h under kinetic control,[26] resulting in a k_H/k_D = 1.0. The lack of kinetic isotope effect indicates that C−H cleavage occurs after the rate-determining step. According to DFT calculations (vide infra), the reaction pathway involves an early transition state where the rate-determining step is dissociation of the cyclooctene ligand to form a 14*e* (PNP)Ir intermediate. Conversion of an η^2_{C-C} benzene complex to an agostic η^2_{C-H} complex involves the second highest barrier, followed by the C−H cleavage step (vide infra).

Reaction of (PNP)Ir(COE)$^+$ (1) with Aryl Halides. When complex **1** was heated in fluorobenzene at 50 °C for 1 h, three regioisomers of (PNP)Ir(H)(C_6H_4F)$^+PF_6^-$ (**7**) were formed. ^{31}P-{^{1}H} NMR revealed signals at 55.2, 58, and 52.3 ppm in a ratio of 2:2:1, assigned to **7a**, **7b**, and **7c**, respectively (vide infra). ^{1}H NMR revealed three signals in the hydride region in the same ratio at −41, −45, and −42.5 ppm, respectively. An NOE experiment was carried out on a mixture of *ortho*- and *para*-isomers (obtained as described below), to assign the observed hydrides and the *ortho*-aryl proton resonances to isomers **7a** and **7c**. Irradiation of the signal at −41 ppm resulted in NOE enhancement of a signal at 7.10 ppm, while irradiation of the signal at −42.5 ppm gave NOE enhancement of the signal at 7.25 ppm corresponding to two protons. Together with H−H correlation spectroscopy (COSY), the signals at −41, −45, and −42.5 ppm were assigned as the *ortho*, *meta*, and *para* C−H-activated fluorobenzene complexes **7a**, **7b**, and **7c**, respectively. Thus, the C−H activation process of fluorobenzene is not selective. Prolonged heating for 48 h at 60 °C resulted in a mixture of the *ortho*-activated and the *para*-activated fluorobenzene complexes **7a** and **7c** in ratio of 1.8:1, respectively. Heating at 70 °C or higher for 48 h resulted in a similar mixture of *o*- and *p*-isomers in a ratio of 2.3:1, respectively (Scheme 6).

Selective C−H activation of fluorobenzene at the *ortho*-position was reported and was studied theoretically as well as experimentally.[15,16,27] The *ortho*-isomer was shown to be the thermodynamically most stable one in the case of a Re complex,[15a] and the kinetically and thermodynamically most stable in the case of Os complex.[15b] Moreover, it is known that the *ortho*-positions in haloarenes are the most acidic ones, especially in fluoroarenes.[28]

(24) (a) Milstein, D. *J. Am. Chem. Soc.* **1982**, *104*, 5227. (b) Milstein, D. *Acc. Chem. Res.* **1984**, *17*, 221. (c) Basato, M.; Longato, B.; Morandini, F.; Bresadola, S. *Inorg. Chem.* **1984**, *23*, 3972. (d) Rosini, G. P.; Wang, K.; Patel, B.; Goldman, A. S. *Inorg. Chim. Acta* **1998**, *270*, 537

(25) *Handbook of Chemistry and Physics*, 57th ed.; CRC Press: Cleveland, OH, 1976.

(26) By kinetic control we mean that there is no significant exchange with benzene in solution under these conditions.

(27) Clot, E.; Besora, M.; Maseras, F.; Mégret, C.; Eisenstein, O.; Oelckers, B.; Perutz, R. N. *Chem. Commun.* **2003,** 490.

(28) Schlosser, M.; Marzi, E.; Cottet, F.; Büker, H. H.; Nibbering, N. M. *Chem. Eur. J.* **2001,** *7*, 3511.

Scheme 6

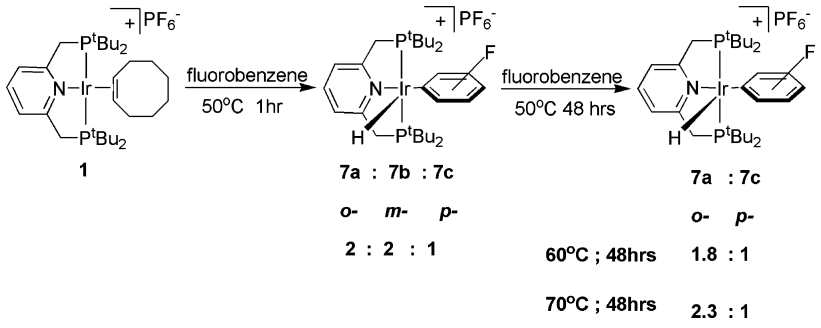

Scheme 7

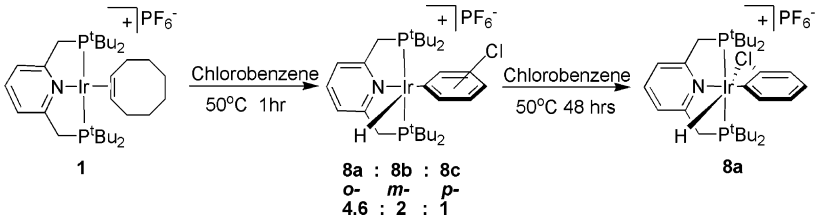

Scheme 8

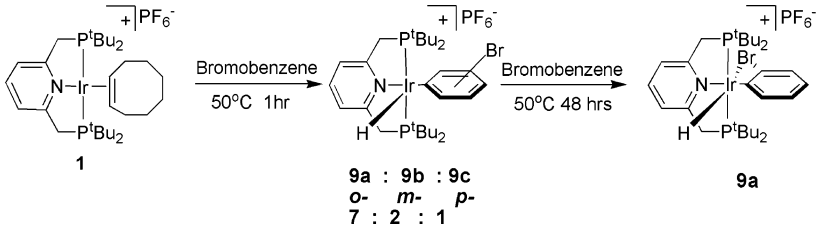

While complex **1** exhibited *no* kinetic preference, and low thermodynamic preference, for the *ortho* C−H bond of fluorobenzene, *ortho* C−H selectivity was observed with chlorobenzene. Thus, heating complex **1** in chlorobenzene at 50 °C for 1 h resulted in the *o*-, *m*-, and *p*-isomers of (PNP)Ir(H)-(C_6H_4Cl) complexes in a ratio of 4.6:2:1, assigned as **8a**−**c**, respectively (vide infra), at a point where **1** was fully consumed (Scheme 7). $^{31}P\{^1H\}$ NMR revealed a signal at 51 ppm corresponding to the *ortho*-isomer and a broad signal at 54 ppm corresponding to the *meta*- and *para*-isomers. ^1H NMR revealed a hydride signal at −34 ppm, which is characteristic of M−*H* *trans* to an occupied coordination site (*ortho*-isomer, see below), and at −41 and −44 ppm for the *meta*- and *para*-isomers. Irradiating the hydride signal in ^1H NMR at −41 ppm gave an NOE enhancement (relative to the aryl protons) at 7.35 ppm. Irradiating the signal at −44 ppm resulted in an NOE enhancement of the aryl protons at 7.45 ppm. Together with COSY data, the signals at −41 and −44 ppm were assigned to the hydride ligands of the *meta* and *para* C−H-activated chlorobenzene complexes **8b** and **8c**, respectively. Monitoring the reaction by NMR revealed at 10% conversion a ratio **8a**:**8b**:**8c** of 4:2:1, indicating that complex **1** has a kinetic preference for the activation of the C−H bond *ortho* to the chlorine atom. Remarkably, when this reaction mixture was heated for 48 h, complex **1** was totally consumed and complexes **8b** and **8c** were *fully converted* to the *ortho*-activated complex **8a** (Scheme 7), indicating that this complex is the most kinetically and thermodynamically favored product under these conditions.

Yellow prismatic crystals were obtained by slow diffusion of pentane into a chlorobenzene solution of complex **8a**. An X-ray analysis of **8a** reveals that the Ir atom is located in the center of a distorted octahedron.[29] The Cl atom is coordinated to the metal, and as predicted from the NMR data, it is located *trans* to the hydride. Although the Ir−Cl bond length of 2.816 Å is significantly shorter than the sum of the van der Waals radii of Ir and Cl atoms, it is longer than other reported Ir−Cl bonds in coordinated chloroalkanes.[12c] This elongation is probably due to some strain in the four-membered ring, as indicated by the Ir−Cl−C angle of 72°. Noteworthy, the C−Cl bond (1.78 Å) is significantly elongated compared to the one in free C_6H_5Cl (1.700 Å),[25] suggesting π-back-donation from a filled metal d-orbital to the empty C−Cl π^*-orbital.

Interestingly, complex **8a** is the most stable isomer despite the steric hindrance imposed by the chlorine atom. The intramolecular coordination of the Cl atom of activated chlorobenzene can explain the higher thermodynamic stability of **8a** versus the other isomers **8b** and **8c**, in which such coordination is impossible. Halocarbon coordination to transition metals is well documented,[12,30] although examples of chloro- and bromoarene coordination are not common.[30] Remarkably, reaction of **1** with bromobenzene is similar to that of chlorobenezene, despite the higher steric hindrance imposed by the Br atom and the expected high reactivity of Ar−Br toward oxidative addition to electron-rich Ir(I) (Scheme 8).

$^{31}P\{^1H\}$ NMR follow-up at 50 °C revealed a signal corresponding to the *ortho* C−H activation complex **9a** at 49 ppm, in addition to a broad signal at 51−51.5 ppm, corresponding to the *m*- and *p*-activated complexes **9b**,**c**. ^1H NMR revealed three hydride signals at −29, −42, and −45 ppm, corresponding to

(29) For detailed crystallographic information see the Supporting Information of ref 17.

(30) (a) Butts, M. D.; Scott, B. L.; Kubas, G. J. *J. Am. Chem. Soc.* **1996**, *118*, 1970. η^1-Coordination of chlorobenzene: (b) Korolev, A. V.; Delpech, F.; Dagorne, S.; Guzei, I. A.; Jordan, R. F. *Organometallics* **2001**, *20*, 3367. (c) Kowalczyk, J. J.; Agbossou, S. K.; Gladysz, J. A. *J. Organomet. Chem.* **1990**, *397*, 333.

Scheme 9

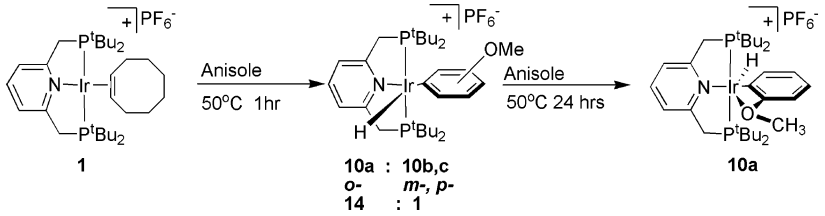

the *ortho*-, *meta*-, and *para*-isomers in a ratio of 7:2:1, respectively, at 10% conversion. Irradiating the signal at −42 ppm resulted in NOE enhancement between the hydride and aryl protons at 7.56 ppm. Irradiating the signal at −45 ppm gave an NOE enhancement between the hydride and aryl proton at 7.52 ppm. Together with COSY results, the signals at −42 and −45 ppm were assigned to the hydride ligands of the *meta* and *para* C−H-activated bromobenzene complexes **9b** and **9c**, respectively. Continued heating at 50 °C for 48 h resulted in quantitative formation of **9a** as the sole product (Scheme 8). These results show that **9a** is both kinetically and thermodynamically favored.

Reaction of (PNP)Ir(COE)$^+$ with Anisole. When **1** was heated in anisole at 50 °C for 1 h, the *ortho*, *meta*, and *para* C−H-activated anisole complexes **10a**−**c** were formed. Complex **10a** was the major product (93% of the resulting mixture). Continued heating for 24 h at the same temperature resulted in the sole formation of the *ortho*-isomer **10a** (Scheme 9). Complex **10a** gives rise to a doublet at 56.60 ppm in the $^{31}P\{^1H\}$ NMR spectrum and a triplet at −42 ppm in the ^1H NMR spectrum.

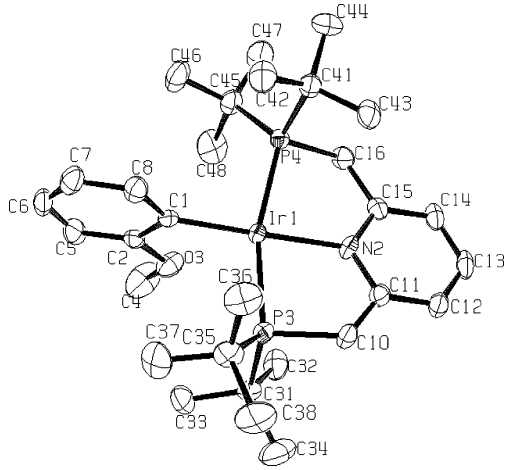

Figure 3. Structure of **10a** (ORTEP drawing, 50% probability level; hydrogen atoms and counteranion are omitted for clarity). For selected bond lengths and angles see Table 3.

Table 3. Selected Bond Lengths and Angles for 10a

selected bond	bond angle (deg)	selected bond	bond length (Å)
N(2)−Ir(1)−P(4)	81.99(10)	Ir(1)−H(1)	1.55(4)
C(8)−C(1)−Ir(1)	131.6(4)	Ir(1)−C(1)	2.038(4)
P(4)−Ir(1)−P(3)	164.04(4)	Ir(1)−P(3)	2.3380(13)
P(3)−Ir(1)−H(1)	90.8(14)	Ir(1)−P(4)	2.3149(13)
C(1)−Ir(1)−P(4)	96.55(13)	Ir(1)−N(2)	2.139(4)
N(2)−Ir(1)−P(3)	83.13(11)	C(2)−O(3)	1.397(6)
N(2)−Ir(1)−C(1)	177.7(17)	O(3)−C(4)	1.425(6)
N(2)−Ir(1)−H(1)	79.5(13)	O(3)−Ir(1)	2.76(2)
C(2)−O(3)−C(4)	116.7(4)		
O(3)−C(2)−C(1)	111.0(4)		
C(5)−C(2)−C(1)	122.6(5)		
C(5)−C(2)−O(3)	126.3(5)		
C(2)−C(1)−Ir(1)	112.5(3)		
C(8)−C(1)−Ir(1)	131.1(2)		
C(8)−C(1)−C(2)	115.9(4)		
P(4)−Ir(1)−H(1)	80.9(14)		
C(1)−Ir(1)−H(1)	102.1(13)		
C(1)−Ir(1)−P(3)	98.48(13)		

Scheme 10

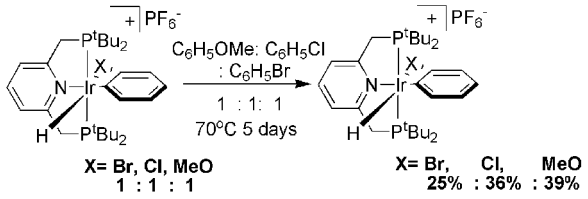

Slow diffusion of pentane into an anisole solution of **10a** resulted in formation of orange prismatic crystals, which were analyzed by X-ray diffraction (Figure 3). Although there is no indication of strong coordination of the oxygen atom to the metal center in **10a** in solution (only −0.22 ppm shift in the ^1H NMR of the OMe group as compared with anisole), there is an indication for directionality toward the metal center in the solid state. Thus, the angles C(8)−C(1)−Ir(1) and C(2)−C(1)−Ir(1) (131.12° and 112.5°, respectively) indicate bending toward the vacant site *trans* to the hydride. This bending is negligible in complex **2**, but very significant in complexes **8a**, **9a**, and **10a**. Moreover, the C(2)−O(3) bond length in the crystal structure (1.397 Å) is longer than the Ar−O bond length of free anisole (1.357 Å),[31] implying interaction of the methoxy group with the metal center.

Exchange Reactions. To compare the regioselective *ortho* C−H activation in chlorobenzene, bromobenzene, and anisole, we have performed competition experiments under conditions in which there is no exchange between the *ortho* C−H-activated complexes **8a**, **9a**, and **10a**. When complexes **8a**, **9a**, and **10a** were dissolved, each one separately, in a mixture of anisole and chlorobenzene (1:1 molar ratio) and heated at 55 °C for 24 h, no reaction took place, indicating that the complexes are kinetically stable under these conditions.

Heating the Ir(I) complex **1** in a mixture of chlorobenzene, bromobenzene, and anisole (1:1:1 molar ratio) at 55 °C for 24 h resulted in a mixture of *ortho*-activated products in a ratio of 38% **10a**, 32% **8a**, and 30% **9a**, indicating only a slight preference toward the *ortho* C−H bond of anisole as compared with haloarenes. No Hammett correlation based on these ratios (which correspond to the relative rates of formation of these complexes) and the σ and the $\sigma+$ constants was found, implying that the overall C−H activation process is not governed by electronic influence. Interestingly, upon heating the *ortho*-activated fluorobenzene complex **7a** at 55 °C for 1.5 h in a mixture of anisole and chlorobenzene at a molar ratio of 1:1, exchange took place, resulting in a mixture of complexes **8a**, **10a**, **8b**,**c**, and **10b**,**c**, after 45% conversion with respect to **7a**.

Heating complexes **8a**, **9a**, and **10a** (1:1:1 molar ratios) in a mixture of anisole:chlorobenzene:bromobenzene (molar ratio of 1:1:1) under thermodynamically controlled conditions, i.e., 70 °C for 5 days,[32] a new mixture of the *o*-isomers was formed.

(31) Seip, H. M.; Seip, R. *Acta Chem. Scand.* **1973**, *27*, 4024.

(32) The ratios were observed after 4 days at 70 °C and were constant for the next 24 h. Moreover, a small amount of C−H activation products resulting from the methoxy group of anisole were observed (23% from the total mixture after 5 days).

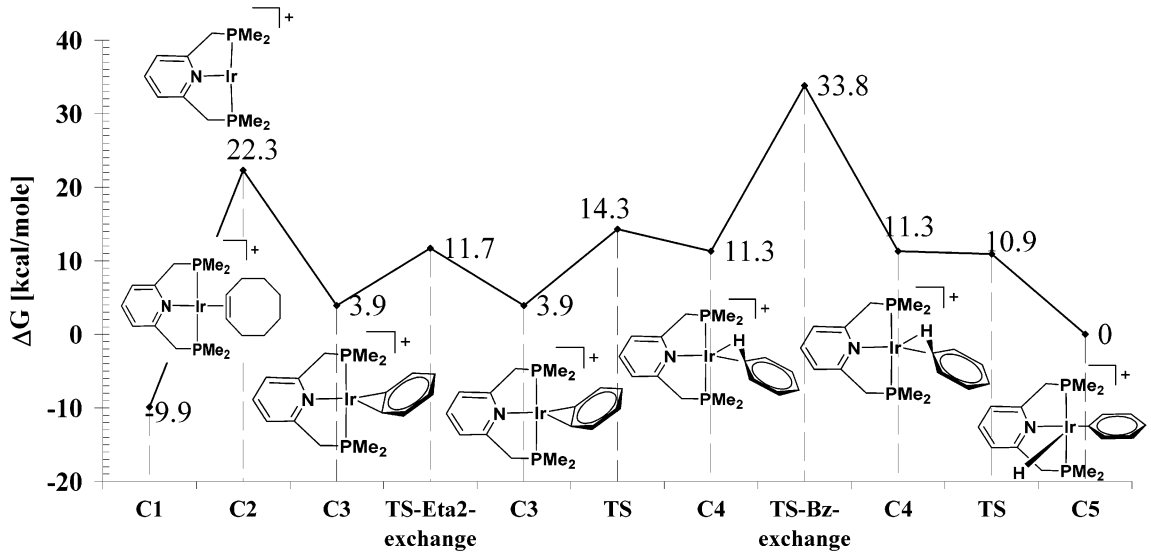

Figure 4. Relative free energies [kcal/mol] for the mechanism of C−H activation of benzene and associative benzene exchange (with benzene) by the (Me-PNP)Ir$^+$ system at the mPW1k/SDD//mPW1k/SDB-cc-pVDZ level of theory.

$^{31}P\{^1H\}$ NMR revealed three signals at 56, 52, and 49 ppm, corresponding to complexes **10a**, **8a**, and **9a,** respectively, in 39%, 36%, and 25%, respectively (Scheme 10). This implies that the anisole- and chlorobenzene-activated complexes **8a** and **10a** are the most stable thermodynamically, with a slight preference to the anisole complex **10a**.

Theoretical Results

To gain further insight into the mechanism of the aryl C−H activation process in the (PNP)Ir(COE)$^+PF_6^-$ (**1**) system, DFT calculations were performed. Geometry optimizations were carried out at the mPW1k/SDD level of theory, and on the optimized structures single-point energy calculation at the mPW1k/SDB-cc-pVDZ level of theory were performed, to increase the accuracy of the results. First, calculations were carried out on the H-PNP(COE)$^+$ system, with no substituents on the phosphine arms, and then, Me substituents were added to the phosphines of the optimized structures in order to simulate better the electronic and steric effects of the realistic system. Finally, where necessary to increase the accuracy of the results, tBu substituents were added and geometry optimization were carried out on the full system at the (mPW1k/LANL2DZ+P//ONIOM(mPW1k/LANL2DZ:mPW1k/LANL1MB)) level of theory. In the calculations we considered three systems: benzene, chlorobenzene, and anisole (PNP)Ir$^+$ systems.

C−H Activation of Benzene by Me-PNP/Ir$^+$. We describe here the mechanism of arene C−H activation by the (Me-PNP)-Ir$^+$ system (a similar mechanism was found for the (H-PNP)-Ir$^+$ system; however, lower barriers were found for the Me system, which is more closely related to the experimental system both electronically and sterically). C−H activation in benzene is also a reference point for further description of C−H activation in chlorobenzene and anisole cases. Both a η^2_{C-H} intermediate and η^2-arene intermediates are implied. The energy profile for the mechanism found for C−H activation in benzene by the (PNP)Ir$^+$ system is described in Figure 4.

Only one reaction sequence leading to the C−H-activated (Me-PNP)Ir(H)(Ph)$^+$ complex **C5** was found (Figure 4). The stepwise arene C−H bond activation starts with an initial dissociation of cyclooctene (COE) to form the T-shaped complex **C2**. Dissociation of COE was found to be the rate-determining step of the reaction, with a dissociation energy of 32 kcal/mol. No transition state was found for the ligand dissociation process. An associative mechanism to generate the η^2-complex from the (PNP)Ir(COE)$^+$ (**C1**) cannot be ruled out: however, no transition state was located for an associative mechanism. After the T-shaped complex **C2** is formed, facile coordination of benzene takes place to form the relatively stable η^2_{C-C} intermediate, **C3**. The η^2_{C-C} arene can easily exchange positions along the aromatic ring with a barrier of 7.8 kcal/mol; however, in the case of benzene this process is degenerate, leading to the same η^2-arene complex, **C3**. To activate the arene C−H bond, complex **C2** should first be converted to the aryl η^2_{C-H} product, **C4**, with a barrier of 10.4 kcal/mol, following by C−H bond activation to form **C5**.[33] No C−H activation was found to take place directly from the arene η^2_{C-C} complex **C3**. The C−H activation product, **C5**, is square pyramidal with the hydride ligand *trans* to an empty coordination site, as in the experimental X-ray structure. It is the thermodynamically most stable product in the system, which can be generated in a stepwise manner from the (PNP)Ir(COE)$^+$ complex **C1** with relatively low barriers. The rate-limiting step in this process was found to be not the C−H activation step but rather the dissociation of the COE ligand from the initial complex to form the highly unstable (PNP)Ir$^+$ T-shaped complex **C2**. From the computational model suggested here it appears that the (PNP)-Ir(COE)$^+$ complex **C1** is more stable than the C−H activation product, (PNP)Ir(Ph)(H)$^+$, **C5**. However, it was shown experimentally that the tBu analogue of complex **C5** is the thermodynamically most stable product of the reaction of (PNP)Ir-(COE)$^+$ with benzene. Thus, to verify the reason for the discrepancy between experimental and computational results, tBu substituents on the phosphines were added to the computational model, and geometry optimizations were carried out for the realistic (tBu-PNP)Ir$^+$ system using the ONIOM two-layer method. Consequently, the results from the ONIOM calculations revealed that the cationic (tBu-PNP)Ir(Ph)(H)$^+$

(33) The transition state leading to **C5** appears to rest below the intermediate, **C4** ($\Delta G^{\ddagger} = -0.4$ kcal/mol). It should be noted that using the mPW1K/SDD-optimized geometry for the mPW1K/SDB-cc-pVDZ energy profile is an approximation that can lead to errors, especially in cases of small energy differences. Furthermore, the correction to the energy used to calculate ΔG_{298} is based upon the rigid rotor harmonic oscillator approximation.

Table 4. Comparison between Selected Bond Lengths (Å) and Angles (deg) of the Calculated and Experimental (X-ray) tBu-PNP/Ir(Ph)(H) Structures

	experimental	calculated
Ir−H	1.66	1.53
Ir−C_{Ph}	2.043	2.027
Ir−N	2.142	2.15
Ir−P	2.32	2.36
C_{Ph}−Ir−H	88	92
N−Ir−H	94	91
N−Ir−C_{Ph}	178	177
P−Ir−P	166	167

complex is more stable than the cationic (tBu-PNP)Ir(COE)$^+$ complex by 8.8 kcal/mol.

Structure of the C−H-Activated Complex 4. The calculated structure of the (tBu-PNP)Ir(Ph)(H)$^+$ complex **4** (tBu derivative of **C5**) (at the mPW1k/LANL2DZ+P//ONIOM(mPW1k/LANL2DZ:mPW1k/LANL1MB level of theory) is in good agreement with the experimental X-ray structure. Comparison between selected bond lengths and angles is presented in Table 4.

Comparison between PNP- and PCP-Ir(Ph)(H) Systems. To address the question of electron density on the Ir(III) complexes, the PCP and PNP complexes (Me-PCP)Ir(Ph)(H) and (Me-PNP)Ir(Ph)(H)$^+$ were calculated and compared for charge densities and bond lengths (see results in Figure 5). It can be seen that the Ir−H bond distance is identical in both systems (1.53 Å). Additionally, the natural charges on both hydrides (+0.13 for both systems) and Ir centers (+0.09 for the PNP and +0.05 for the PCP) are comparable. Thus, the nature of the H ligand is similar in the two systems (i.e., hydridic), and the complex is Ir(III) both for PNP and PCP systems. However, when comparing the Ir−Ph bonds, it can be seen that in the PCP system the Ir−C_{Ph} bond length is 0.06 Å longer (2.09 Å) than in the PNP system (2.03 Å). Similarly, the C_{ipso}−Ir bond in the (PCP)Ir system is 0.06 Å shorter than the analogous N−Ir in the (PNP)Ir$^+$ system. Similar results were obtained when comparing the realistic (tBu-PCP)Ir and (tBu-PNP)Ir$^+$ systems (Figure 5). Similar bond lengths and angles for the (PCP)Ir system were obtained by Krogh-Jespersen *et al.*[46] in calculations using the B3LYP functional. Thus, it can be suggested that in both systems the C−H activation reaction

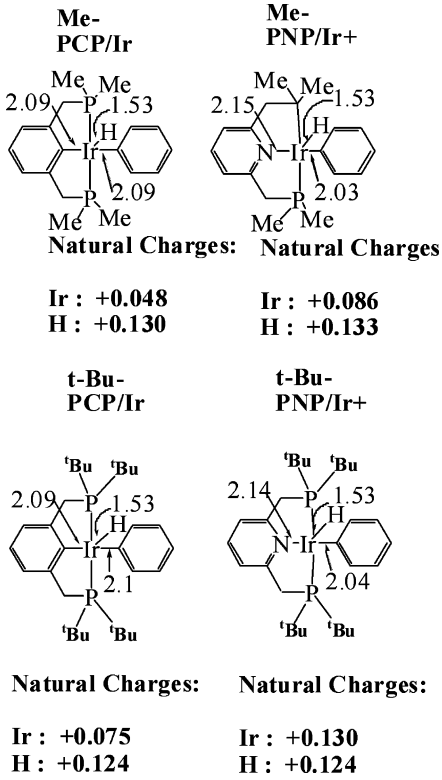

Figure 5. Comparison between selected NPA (natural population analysis) charges and bond lengths (Å) of the (PNP)Ir(Ph)(H)$^+$ and the (PCP)Ir(Ph)(H)$^+$ systems (Me and tBu substituents on the phosphines).

is oxidative, leading to the formation of Ir(III) complexes. The *trans* effect of the PCP-aryl groups is probably responsible for the elongation and weakening of the Ir−C_{ipso} bond *trans* to it. This effect lowers the overall stability of the (PCP)Ir(H)Ph complex in comparison to the (PNP)Ir(H)Ph$^+$ system.

C−H Activation of Chlorobenzene by (Me-PNP)Ir$^+$. The C−H activation process of chlorobenzene is expected to have a mechanism similar to the one found for benzene C−H activation. However, in contrast to benzene, in chlorobenzene there are three choices for C−H activation, leading to the formation of three metal aryl complexes, *ortho*, *para*, and *meta* to Cl. There is also a possibility of C−Cl activation in this system. The experimental work shows a remarkable preference for the *ortho*-Cl position C−H activation both kinetically and thermodynamically. The kinetic reason for this discrimination is suggested to be precoordination of the halide to the metal center, directing the activation toward the *ortho*-position of the arene. The thermodynamic preference is, at least partially, a result of stabilization of the *ortho* C−H-activated complex by additional coordination of the halide to the metal center, as observed in the X-ray structure of the product.[17] DFT calculations were performed in order to address both the kinetic and the thermodynamic issues. The analysis of the computational

(34) The six different η^2-arene complexes (**11**, **9**, **18**, and **10**) can be viewed as three pairs of enantiomers (**18** and **10**; **9** (*ortho*); **11** (*meta*)). In the case of *meta* (**11**) and *ortho* (**9**), each one of the η^2-arene complexes can lead to two different η^2_{C-H} complexes since the metal center can equally reach both C−H bonds of the two coordinated carbons. To avoid complication, we chose all the η^2-complexes to be different (by giving them different numbers) and each one to lead to only one η^2_{C-H} complex (with η^2-arene complex **10** not leading to any η^2_{C-H} complex).

(35) TSs for association and dissociation of ligands are generally difficult to locate on the bottom-of-the-well energy surface, as the maximum on the finite-temperature free energy surface is often purely entropic in origin, unless significant geometric rearrangement is involved.

(36) C−H activation in the methoxy group is beyond the scope of this study.

(37) No transition state was located for this rotation around the Ir−C bond; however, it is expected to be low in energy. The experimental results support the assumption that this rotation barrier is low since only one *meta* and one *ortho* C−H activation complex were observed by NMR, suggesting that the rotation between the isomers is facile.

(38) Hall, C.; Perutz, R. N. *Chem. Rev.* **1996**, *96*, 3125.

(39) (a) Lavin, M.; Holt, E. M.; Crabtree, R. H. *Organometallics* **1989**, *8*, 99. (b) Toner, A. J.; Grundemann, S.; Clot, E.; Limbach, H. H.; Donnadieu, B.; Sabo-Ettienn, S.; Chaudret, B. *J. Am. Chem. Soc.* **2000**, *122*, 6777.

(40) Vigalok, A.; Uzan, O.; Shimon, L. W. J.; Ben-David, Y.; Martin, J. M. L.; Milstein, D. *J. Am. Chem. Soc.* **1998**, *120*, 12539.

(41) Rybtchinski, B.; Cohen, R.; Martin, J. M. L.; Milstein, D. *J. Am. Chem. Soc.* **2003,** *125*, 11041.

(42) Rybtchinski, B.; Oevers, S.; Montag, M.; Vigalok, A.; Rozenberg, H.; Martin, J. M. L.; Milstein, D. *J. Am. Chem. Soc.* **2001,** *123*, 9064.

(43) Collman, J. P.; Hegedus, L. S.; Norton, J. R.; Finke, R. G. *Principles and Applications of Organotransition Metal Chemistry*; University Science Books: Mill Valley, CA, 1987.

(44) Zhu, K. M.; Achord, P. D.; Zhang, X. W.; Krogh-Jespersen, X. W.; Goldman, A. S. *J. Am. Chem. Soc.* **2004**, *126*, 13044.

(45) Since the associative mechanism for arene exchange is affected by the steric hindrance of the ligands, it is anticipated that for the realistic system (tBu-PNP/Ir) this barrier will be even higher in energy than the one for the computed Me-PNP/Ir system.

(46) Krogh-Jespersen, K.; Czerw, M.; Kanzelberger, M.; Goldman, A. S. *J. Chem. Inf. Comput. Sci.* **2001**, *41*, 56.

a)

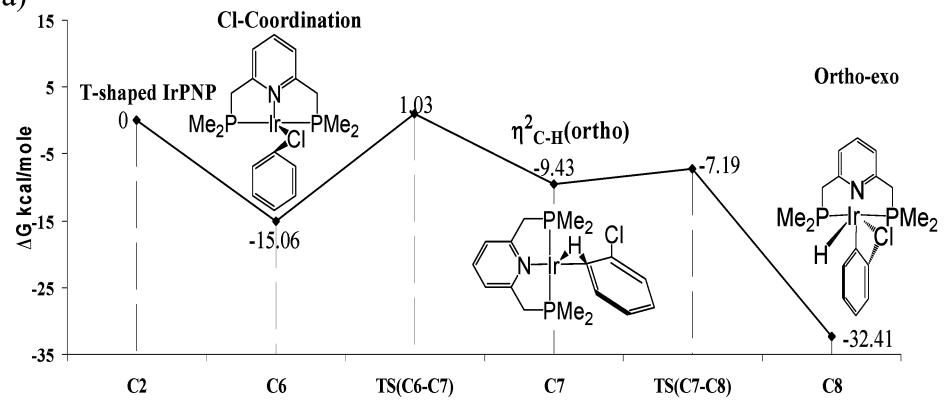
Cl-Coordination
T-shaped IrPNP
Ortho-exo
ΔG kcal/mole
15
5
-5
-15
-25
-35
0
-15.06
1.03
η2C-H(ortho)
-9.43
-7.19
-32.41
C2
C6
TS(C6-C7)
C7
TS(C7-C8)
C8

b)

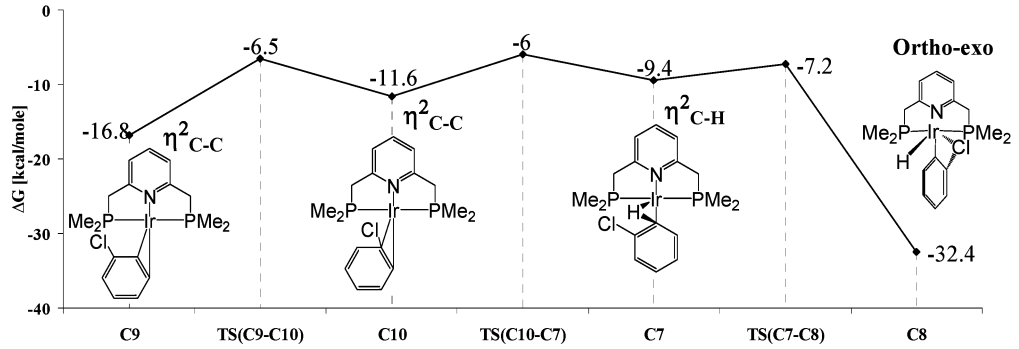
ΔG [kcal/mole]
0
-10
-20
-30
-40
-16.8
η2C-C
-6.5
-11.6
η2C-C
-6
η2C-H
-9.4
-7.2
Ortho-exo
-32.4
C9
TS(C9-C10)
C10
TS(C10-C7)
C7
TS(C7-C8)
C8

c)

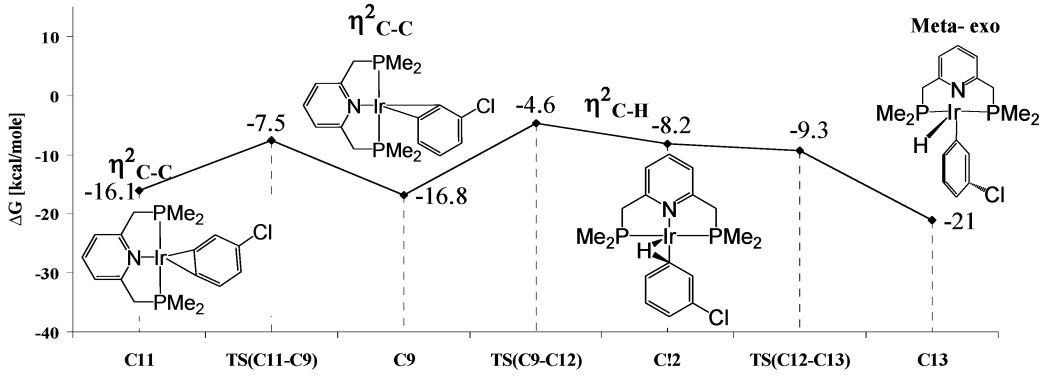
ΔG [kcal/mole]
10
0
-10
-20
-30
-40
η2C-C
-16.1
-7.5
η2C-C
-16.8
-4.6
η2C-H
-8.2
-9.3
Meta- exo
-21
C11
TS(C11-C9)
C9
TS(C9-C12)
C!2
TS(C12-C13)
C13

d)

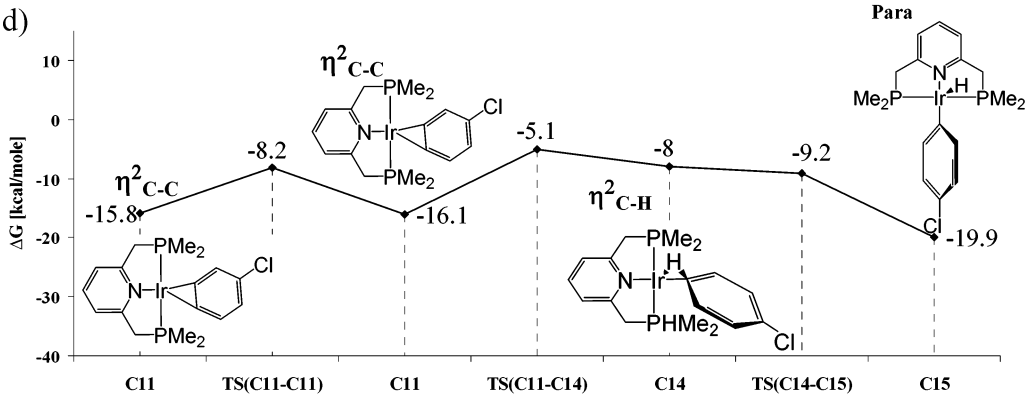
ΔG [kcal/mole]
10
0
-10
-20
-30
-40
η2C-C
-15.8
-8.2
η2C-C
-16.1
-5.1
η2C-H
-8
-9.2
Para
-19.9
C11
TS(C11-C11)
C11
TS(C11-C14)
C14
TS(C14-C15)
C15

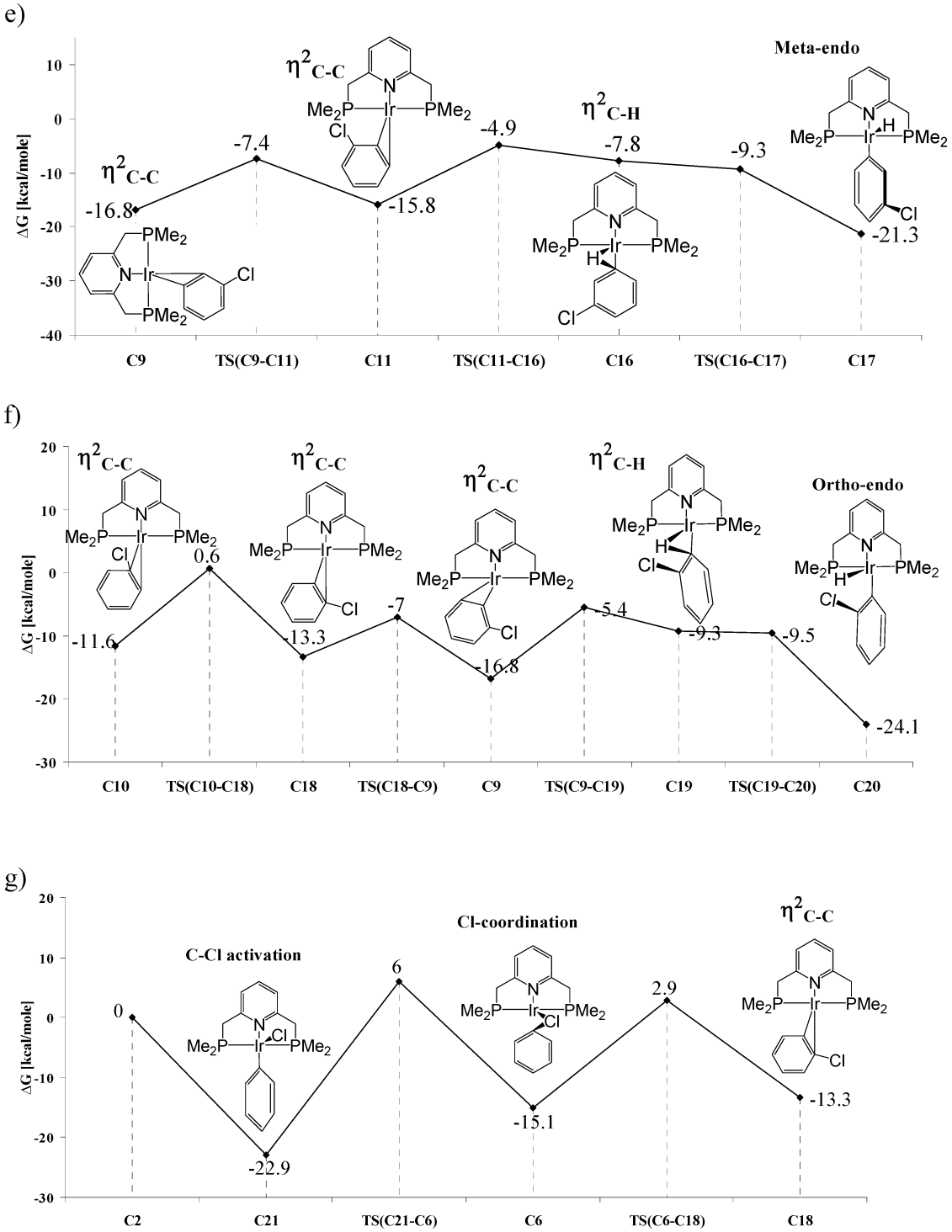

Figure 6. Detailed graphs, each representing a distinct pathway for the formation of the different C−H activation products (*ortho*, *meta*, or *para* conformers) including an interchange pathway leading from one η^2-arene complex to a different η^2-arene one.

results describes the mechanism of C−H activation in chlorobenzene taking into account all the possible isomers of the C−H-activated complexes and intermediates involved. On the basis of the mechanistic study we interpret the experimental results also taking the possibility of C−Cl activation into account. As in the benzene system, geometry optimizations were first carried out on the (H-PNP)Ir(H)$(C_6H_4Cl)^+$ system at the mPW1k/SDD level of theory, then Me substituents were added to the optimized geometries and the structures were reoptimized. On these optimized geometries, single-point energies were calculated at the mPW1k/SDB-cc-pVDZ level of theory in order to increase the accuracy of the results. The mechanism of C−H activation in chlorobenzene mediated by the (Me-PNP)Ir^+ system was found to be similar to the one in benzene. However, it should be noted that in addition to the different isomers of C−H-activated complexes (two *ortho* C−H isomers, two *meta* C−H isomers, and one *para* C−H isomer) obtained in the C−H activation process of chlorobenzene, it involves also different isomers for the intermediates. Thus, there are five isomers for η^2_{C-H} complexes, four isomers for η^2-arene complexes,[34] and various transition states connecting between them. Consequently, five pathways were found for C−H activation taking place from η^2-complexes, one pathway found for C−H activation taking

place from a Cl-coordinated complex, and one pathway was found for C−Cl activation. Detailed graphs are given in Figure 6.

The C−H activation of chlorobenzene proceeds, as in benzene C−H activation, through the formation of a η^2_{C-H} complex, leading to the corresponding C−H-activated complex. However, since there are five different η^2_{C-H} complexes, each of the five could be obtained from a distinct η^2-arene complex or, in the case of *ortho*-η^2_{C-H} complex **C7**, also from the Cl-coordinated complex **C6**. In contrast to the degenerate η^2-arene site interchange process in benzene, here each site interchange (out of six different ones) leads eventually to a different C−H activation isomer, since there is only one η^2_{C-H} complex that could be formed from each η^2-arene complex.[34] The η^2-arene complexes are directing the metal center toward the C−H bond to be cleaved, since precoordination of the arene is necessary to bring the C−H bond into close proximity to the metal center. However, where chlorobenzene is concerned, the Cl-coordinated complex **C6** could also play a role in predirecting to C−H activation in the *ortho*-position of chlorobenzene (vide infra).

It can be clearly seen from Figure 6 that both *ortho* C−H activation products (**C8** and **C20**) are the thermodynamically most stable products and that the *exo*-isomer complex **C8**, with the Cl moiety coordinated to the metal center, is substantially more stable than the rest of the isomers (by 8−12 kcal/mol), explaining the experimentally observed thermodynamics preference of the *ortho*-Cl isomer. The rotation around the Ir−C bond to convert between the two computationally found *ortho*-isomers **C8** and **C20** is expected to have a very low barrier, and no transition state was located for this rotation. The experimental results support the assumption that this rotation barrier is low since only one *meta* and one *ortho* C−H activation complex were observed by NMR, suggesting that the rotation between the isomers is facile. In general, the more stable isomer is observed.

We considered also a possibility of C−Cl oxidative addition. The C−Cl-activated complex **C21** is about 9.5 kcal/mol less stable than the *ortho* C−H activation complex **C8**. This is most likely due to the lack of stabilization by additional coordination to the empty site of the metal center of complex **C21**, as in the C−H-activated complex **C8**. ONIOM calculations of the tBu derivatives of the *ortho*-C−H and the C−Cl-activated complexes support the conclusion that indeed the (tBu-PNP)Ir(H)(C_6H_4-Cl)$^+$ complex is more stable than the (tBu-PNP)Ir(Cl)(Ph)$^+$ (by 7.5 kcal/mol).

Based on the DFT calculations, the C−Cl activation complex **C21** has thermodynamic stability similar to that of other C−H-activated complexes observed transiently in the experimental system (*meta* and *para* C−H activation isomers, **C13**, **C17**, and **C15**); however, it was not observed experimentally. Thus, the reason that complex **C21** was not observed is probably kinetic rather than thermodynamic. To understand the kinetics of its formation, the transition states leading to the C−Cl- and the C−H-activated complexes were compared. C−Cl bond activation was found to take place exclusively and directly from the Cl-coordinated complex **C6**. No direct activation of the C−Cl bond was found to take place either from an η^2-complex such as **C10** or **C18** or from an *ortho*-Cl η^2_{C-H} complex such as **C7** or **C19**. Thus, to cleave the C−Cl bond, the Cl-coordinated complex **C6** should first be formed. After its generation, complex **C6** can follow three pathways (Figure 6): (a) oxidative addition of the C−Cl bond to form complex **C21** (with a barrier of $\Delta G^{\ddagger} = 21$ kcal/mol); (b) formation of the η^2-arene complex **C18** with a lower barrier ($\Delta G^{\ddagger} = 18$ kcal/mol), which can react further to give eventually the *endo*-*ortho*-C−H-activated complex **C20**; or (c) formation of the *ortho*-η^2_{C-H} complex, **C7**, with a lower barrier of $\Delta G^{\ddagger} = 16$ kcal/mol, leading directly to the most stable *ortho*-C−H activation complex **C8**.

Since the pathway leading to the C−Cl activation complex has the highest barrier of all three, it is the most improbable one to occur. Therefore, as the Cl-coordinated complex **C6** is formed, it will most likely follow the C−H activation pathway rather than the C−Cl activation one, supporting the experimental results. In the (Me-PNP)Ir$^+$ system there is no significant thermodynamic preference for formation of the Cl-coordinated complex **C6** over formation of other Ir(I) arene complexes, especially the η^2-arene species, which have stability comparable to that of **C6**. Nevertheless, it is expected that as the bulk around the metal center increases, the more sterically demanding η^2-arene intermediates will become less stable with respect to the less sterically hindered Cl-coordinated intermediate. To verify this postulation, the stability of the Cl-coordinated complex **C6** with respect to the η^2-arene intermediates should be calculated for the realistic system. Thus, ONIOM calculations of the tBu analogues of complexes **C6** and **C9** were performed. Consequently, it was found that for the (tBu-PNP)Ir$^+$ system the Cl-coordinated complex is more stable than the η^2-arene one (the analogue of the most stable η^2-arene for the (Me-PNP)Ir$^+$ model system, complex **C9**) by 12.7 kcal/mol. Thus, the Cl-coordinated complex in the realistic system is substantially more stable than the rest of the Ir(I) intermediates, probably due to reduced steric interference in the case of Cl coordination, in comparison to the η^2-arene complex. Therefore it is the most probable one to be formed in higher concentrations in the experimental system. As a result, the lowest barrier pathway taking place from the Cl-coordinated complex **C6** leading to the *ortho*-η^2_{C-H} complex **C7** might explain also the kinetic preference observed experimentally for the *ortho*-C−H complex **C8**. Thus, when the Cl-coordinated complex is formed, it might lead to the formation of the *ortho* C−H-activated complex. Therefore, coordination of chlorobenzene to the metal center via the halide may result in the selective *ortho* C−H bond oxidative addition with no formation of the C−Cl activation product during the reaction. No TS was located for the formation of the Cl-coordinated complex from the T-shaped (PNP)Ir$^+$ (or from any other intermediate), but it is expected to have a lower barrier than for the formation of an η^2-arene complex since the product is less sterically hindered and less geometrically constrained.[35]

As can be seen from Figure 6, the kinetic barriers for η^2-arene to η^2-arene interchange, η^2-arene to η^2_{C-H}, and C−H activation reactions are similar for all the five different pathways leading to the C−H activation products from the η^2-arene complexes. The highest barrier in each of the five similar pathways is the formation of the η^2_{C-H} bond from the corresponding η^2-arene complex. These barriers are all around 11 kcal/mol, with the smallest TS (**C10**−**C7**) barrier of 6 kcal/mol being the one that leads to the formation of *ortho*-η^2_{C-H} complex **C7**. This probably results from the relatively unstable η^2-arene complex **C10**, preceding the formation of **C7** (probably due to a steric interference between the Cl atom and the phosphine ligand).[34] The interchange barriers between any two η^2-arene complexes are also similar (∼8−10 kcal/mol) with the exception of one slightly higher barrier ($\Delta G^{\ddagger} = 12$ kcal/mol), corresponding to interchange between the two most sterically hindered η^2-arene conformers **C10** and **C18** (Figure 6f). Thus, essentially all the sites on the Cl-benzene ring are kinetically accessible for coordination through an η^2-arene interchange and conversion to the corresponding η^2_{C-H} complexes. Conse-

Table 5. Comparison between Selected Bond Lengths (Å) and Angles (deg) of the Calculated and Experimental Structure of the *ortho*-Cl C−H Activation Complex

	X-ray	mPW1k
Ir−Cl	2.816	2.812
Ir−H	1.524	1.534
Ir−C_1	2.045	2.026
Ir−N	2.159	2.119
C_2−Cl	1.78	1.857
Ir−P	2.33	2.39
C_{Ar}−Ir−H	103	96.2
N−Ir−H	82	91.07
Ir−Cl−C_2	72	71.74
Cl−Ir−C_{Ar}	63.84	65.5

quently, all the sites can be activated with relatively small barriers. Furthermore, the back reaction barriers (C−H reductive elimination) from all C−H-activated complexes apart from **C7** ($\Delta G^{\ddagger} = 25.2$ kcal/mol) are low as well ($\Delta G^{\ddagger} \approx 10-15$ kcal/mol). Thus, in the case of *meta* and *para* C−H-activated complexes (**C17**, **C13**, and **C15**), the microscopic reverse reaction, C−H reductive elimination, can take place and by subsequent transformations can eventually lead to the formation of the most stable product **7**. This *ortho* C−H-activated complex may be regarded as a thermodynamic sink since the C−H reductive elimination from it is much higher in energy than any other transformation in the system including the C−H reductive elimination from other C−H-activated complexes (**C13**, **C15,** **C17**, and **C20**).

Structure of the *ortho*-Cl C−H Activation Complex. The tBu derivative of complex **C8** was calculated by the ONIOM method at the mPW1k/LANL2DZ+P//ONIOM(mPW1k/LANL2DZ:mPW1k/LANL1MB) level of theory. The resulting structure is in good agreement with the experimental X-ray structure.[17] Comparison between selected bond lengths and bond angles of the calculated and the experimental structures can be seen in Table 5.

Our computational system is in good agreement with the experimental one regarding the kinetics and the thermodynamics of the chlorobenzene reaction with the cationic (PNP)Ir^+ system. The computational study suggests a mechanism involving the formation of different isomers of η^2-arene and η^2_{C-H} complexes eventually leading to the thermodynamically most stable *ortho*-Cl C−H activation complex **C8**.

C−H Activation of Anisole by Me-PNP/Ir^+. Anisole exhibits experimentally thermodynamic and kinetic preference for the formation of an *ortho*-methoxy-C−H activation complex, as in the case of chlorobenzene. To assess the mechanism of such selectivity, we investigated computationally the arene C−H activation in anisole.[36] As in the chlorobenzene system, geometry optimizations were first carried out on the H-(PNP)-Ir(anisol)$^+$ system at the DFT mPW1k/SDD level of theory, then Me substituents were added and the structures were reoptimized. Single-point energies were calculated on the optimized geometries at the mPW1k/SDB-cc-pVDZ level of theory to increase the accuracy of the results.

The arene C−H activation of anisole is very similar to the one of chlorobenzene, involving multiple isomers of intermediates and transition states. Detailed graphs for each C−H activation site are presented in Figure 7.

In agreement with the experiment, the *ortho*-methoxy C−H-activated complex **C27** was found to be the thermodynamic product, stabilized by 6−10 kcal/mol relative to the other C−H activation complexes. The kinetics observed for C−H activation processes in anisole is similar to that found for chlorobenzene. The highest barriers are the ones leading from the O-coordinated complex to η^2_{C-C} or η^2_{C-H} complexes ($\Delta G^{\ddagger} \approx 15$ kcal/mol). Slightly lower barriers were found for the formation of the η^2_{C-H} complexes from the η^2-arenes (8−12 kcal/mol high). All η^2_{C-H} complexes have similar stability; the same is true for the η^2-arene complexes, with the exception of the sterically hindered *endo* (**C25**) and *exo* (**C28**) η^2-arenes, which are about 5 kcal/mol higher in energy than the others. In these η^2-arene complexes the steric repulsion between the methoxy moiety and the phosphine ligand is influencing the relative stability of the complexes. The barriers for transforming from one η^2-arene complex to another are also relatively low (4−8 kcal/mol, with the exception of the ones leading to the formation of the sterically hindered η^2-arenes), similarly to those in the chlorobenzene activation profile. The lowest barriers found for the C−H oxidative addition take place from the η^2_{C-H} complexes ($\Delta G^{\ddagger} < 2$ kcal/mol).

Considering the kinetics, as in the chlorobenzene case, in the Anisole system, too, the direct pathway leading from the O-coordinated complex **C22** to the *ortho* η^2_{C-H} complex **C23** is kinetically accessible ($\Delta G^{\ddagger} = 14.7$ kcal/mol) and lower than the alternative one leading from **C22** to the η^2-arene complex **C25** ($\Delta G^{\ddagger} = 17.0$ kcal/mol). Similarly to the chlorobenzene system, in the calculated (Me-PNP)/Ir model system, the O-coordinated complex **C22** appears to be less stable than most of the η^2-arene complexes (**C29**, **C30**, **C33**, and **C36**). To verify the stability of the O-coordinated complex relative to the η^2-arene complexes in the realistic system, we carried out ONIOM calculations on the tBu-substituted analogues of complexes **C22** and **C30** (which is the most stable η^2-arene complex). It was found that the O-coordinated complex is *more stable* than the t-Bu η^2-arene analogue of **C30** by 7.7 kcal/mol (while in the Me-PNP system it is less stable by 3 kcal/mol). The significant stabilization of the O-coordinated complex with respect to the η^2-arene one will most probably result in much higher concentration of this intermediate in the reaction mixture. At the actual experimental conditions (heating to 70 °C), the barrier leading from the O-coordinated complex **C22** to the η^2_{C-H} complex **C23** ($\Delta G^{\ddagger} = 14.7$ kcal/mol) can be overcome. Accordingly, since the O-coordinated complex can preferentially lead to the formation of the *ortho* η^2_{C-H} complex **C23**, the formation of the corresponding *ortho* C−H activated complex **C24** might be kinetically favored over the formation of the rest of the isomers. The Ir−C_{Ar} bond in this *endo*-isomer can be rapidly rotated to give the thermodynamically most stable product **C27**.[37] The slightly higher energy pathway taking place from the O-coordinated complex **C22**, leading to an η^2-arene complex **C25**, will preferentially lead to the formation of **C27** as well and may contribute to its kinetic preference over the other isomers of the C−H activation complexes.

Structure of the *ortho* C−H Activated Complex. A comparison between the X-ray structure of the *ortho*-methoxy C−H activated anisole complex and the calculated ones at two levels of theory is presented in Table 6. The computed structure of (tBu-PNP)Ir(H)(C_6H_4OMe)$^+$ (calculated at the ONIOM-(mPW1k/LANL2DZ:mPW1k/LANL1MB) level of theory) closely resembles the experimental X-ray structure. The Ir−X (X = H, N, P) bond lengths are similar to those found by X-ray analysis, although the Ir−O bond is slightly shorter in the computed structure than the X-ray one (2.60 vs 2.76 Å). Nevertheless, as in the X-ray structure, the methoxy group in the computed structure is not directly coordinated to the Ir atom but rather directed toward it. To confirm that the oxygen atom is not coordinated to the Ir center, an additional calculation of this structure using a different functional (ONIOM(B97-1/

a)

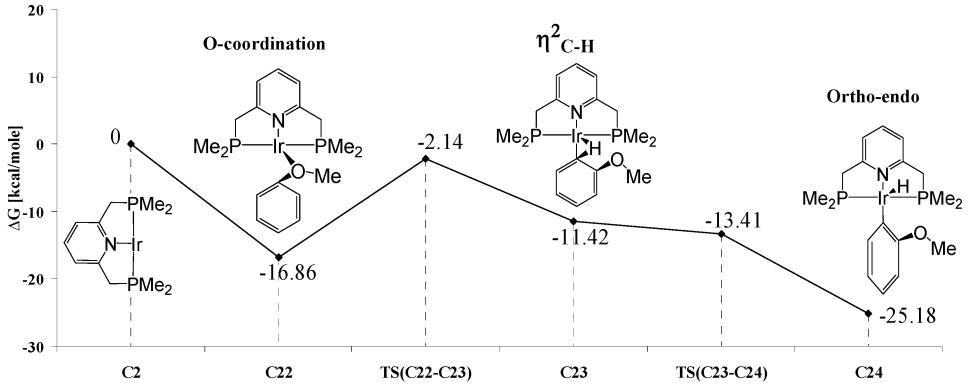
O-coordination
η2C-H
Ortho-endo
ΔG [kcal/mole]
0
-16.86
-2.14
-11.42
-13.41
-25.18
C2
C22
TS(C22-C23)
C23
TS(C23-C24)
C24

b)

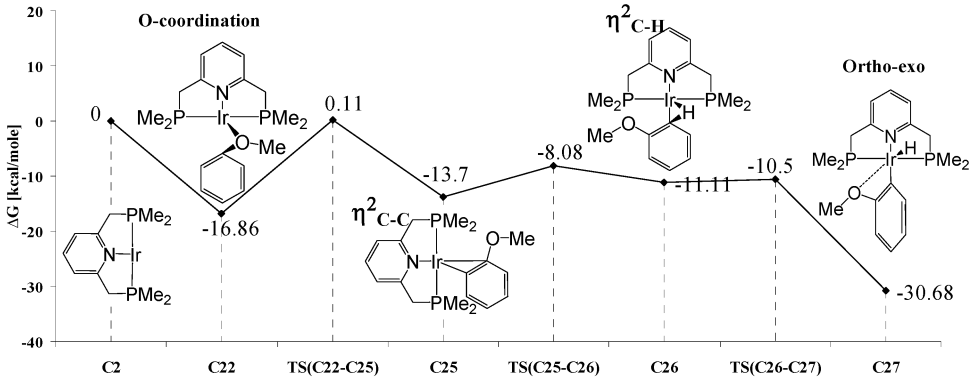
O-coordination
η2C-H
Ortho-exo
η2C-C
ΔG [kcal/mole]
0
-16.86
0.11
-13.7
-8.08
-11.11
-10.5
-30.68
C2
C22
TS(C22-C25)
C25
TS(C25-C26)
C26
TS(C26-C27)
C27

c)

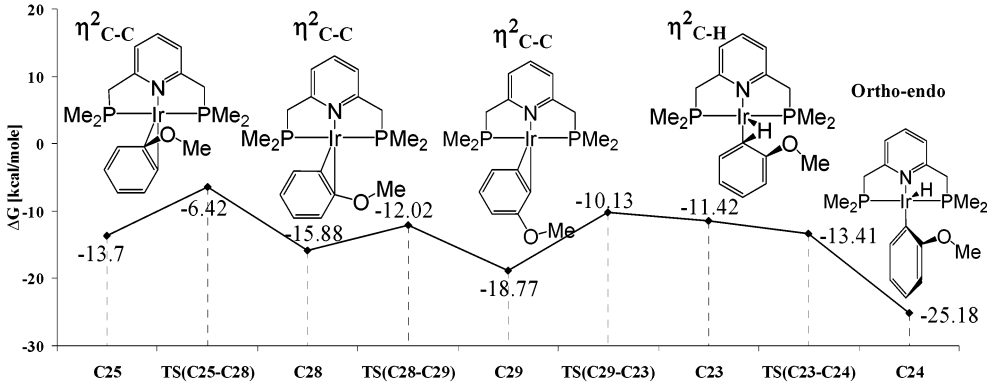
η2C-C
η2C-C
η2C-C
η2C-H
Ortho-endo
ΔG [kcal/mole]
-13.7
-6.42
-15.88
-12.02
-18.77
-10.13
-11.42
-13.41
-25.18
C25
TS(C25-C28)
C28
TS(C28-C29)
C29
TS(C29-C23)
C23
TS(C23-C24)
C24

d)

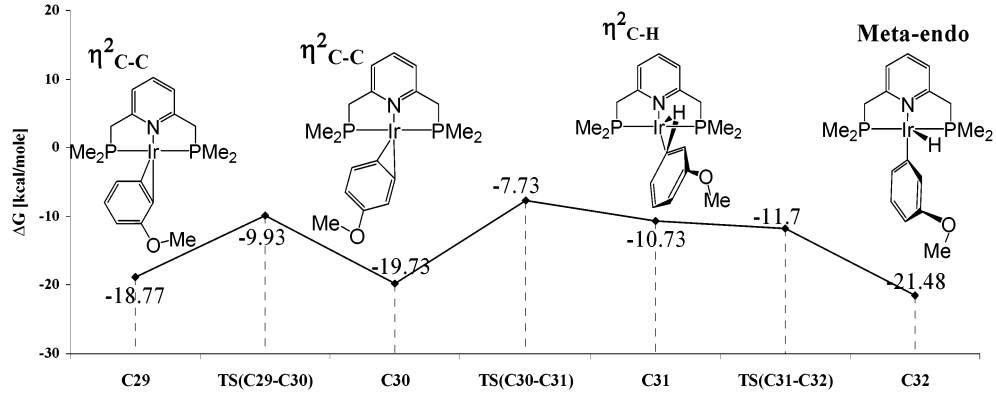
η2C-C
η2C-C
η2C-H
Meta-endo
ΔG [kcal/mole]
-18.77
-9.93
-19.73
-7.73
-10.73
-11.7
-21.48
C29
TS(C29-C30)
C30
TS(C30-C31)
C31
TS(C31-C32)
C32

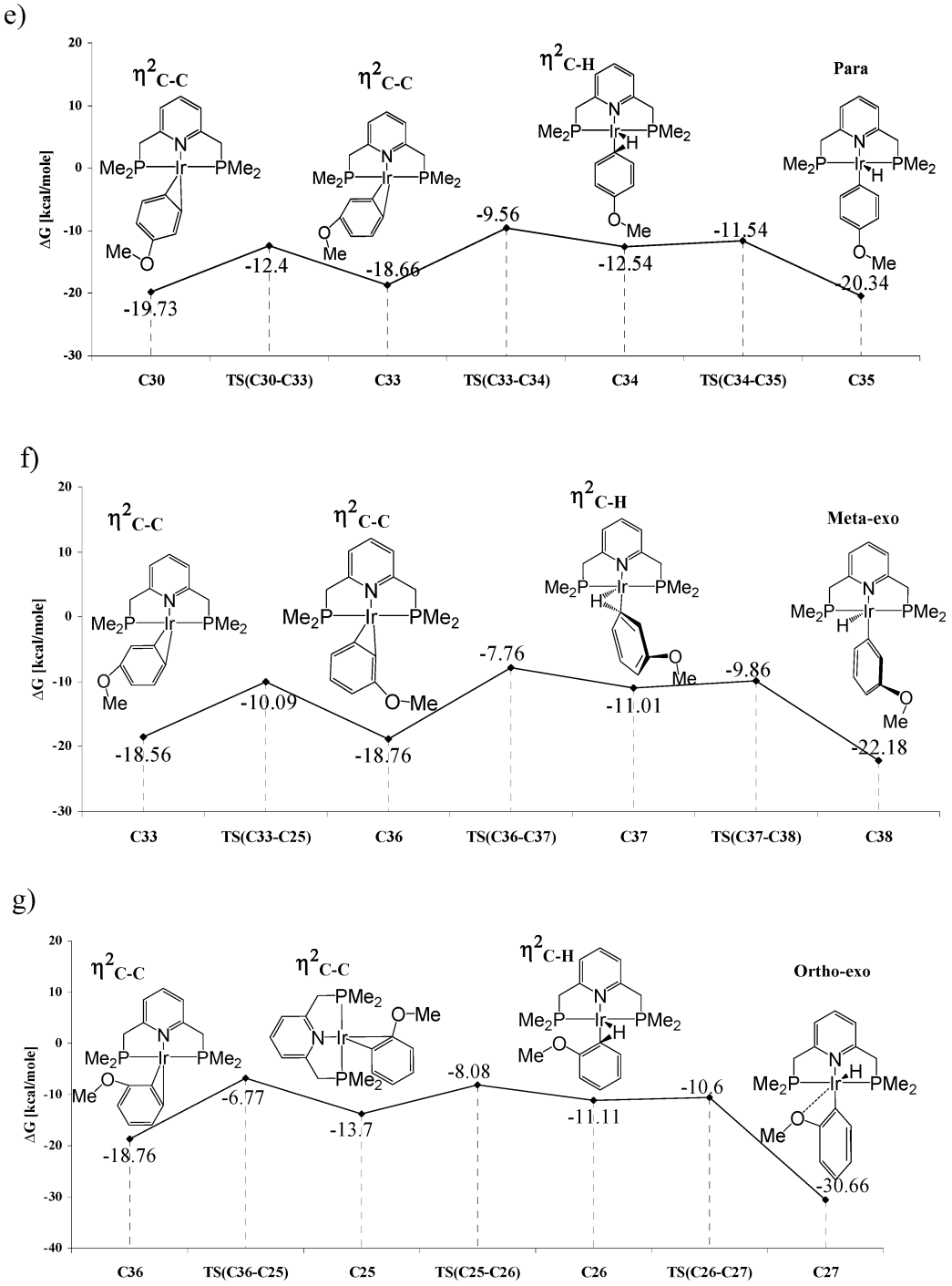

Figure 7. Detailed graphs, each representing a distinct pathway for the formation of the different C−H activation products (*ortho*, *meta*, or *para* conformers) including a site exchange pathway leading from one η^2-arene complex to a different η^2-arene one.

LANL2DZ:B97-1/LANL1MB) level of theory) was performed. Consequently, a longer Ir−O bond distance of 2.92 Å was computed at this level of theory, confirming that the methoxy moiety is not coordinated to the metal center. However, the methoxy group might interact electrostatically with the metal center (δ^+ on Ir, δ^- on O), stabilizing the *ortho*-isomer with respect to other C−H activated isomers due to closer proximity of the methoxy moiety to the metal center. Natural bond order (NBO) calculations confirm that the oxygen atom is not coordinated to the metal center (Wiberg index of 0.028 for the Ir−O bond with respect to a larger 0.105 index for the Ir−Cl bond in chlorobenzene aryl hydride complex). Based on the natural population analysis (NPA) the partial charge on the oxygen atom is −0.625, whereas on the Ir center it is +0.175, compared to a smaller charge of −0.086 on the Cl atom and +0.157 on the Ir in the analogous chlorobenzene complex.

Comparison between C−H Activation of Anisole, Chlorobenzene, and Benzene. Comparing the analogous isomers of C−H activation of chlorobenzene and anisole (*ortho-exo*, *ortho-endo*, *meta-exo*, *meta-endo*, and *para*), it can be seen in general that their stability is similar (within 1 kcal/mol). The anisole C−H activated complexes are slightly more stable than the analogous chlorobenzene ones, apart from the *ortho-exo* complexes, for which the chlorobenzene complex is slightly more stable. This stability is probably gained by the stronger coordination of the chlorine atom than of the oxygen atom to the metal center. This is also supported by NBO calculations, showing larger bond order for Ir−Cl than Ir−O (vide supra).

Table 6. Comparison between Selected Bond Lengths (Å) and Angles (deg) for the Calculated and the X-ray Structures for the *ortho*-tBu-PNP/Ir(H)(Ar) (Ar = $C_6H_4OCH_3$) Complex[a]

	exptl (X-ray)	calcd (mPW1k)	calcd (B97)
Ir−O	2.762	2.599	2.917
Ir−H	1.553	1.532	1.539
Ir−C_{ipso}	2.038	2.025	2.048
Ir−N_2	2.138	2.131	2.164
P_1−Ir	2.317	2.371	2.395
P_2−Ir	2.315	2.375	2.403
C_2−O	1.397	1.417	1.435
O−Me	1.425	1.444	1.469
Ir−P	2.338	2.373	2.399
P−Ir−P	164.06	163.27	164.86
C_{ipso}−Ir−N_2	177.7	174.86	178.18
Ir−C_{ipso}-C_2	112.5	108.37	115.89
C_2−O−Ir	81.08	82.94	77.53
O−Ir−C_{ipso}	55.4	58.46	53.86

[a] Calculated structures are at the mPW1k/LANL2DZ+P//ONIOM(mPW1k/LANL2DZ:mPW1k/LANL1MB) and the B97-1/LANL2DZ+P//ONIOM(B97-1/LANL2DZ:B97-1/LANL1MB) levels of theory.

The stability of the benzene C−H activation product is comparable to the *ortho-endo*-, *meta*-, and *para*-isomers of anisole and chlorobenzene, but it is lower than the stability of the *ortho-exo* complexes, probably due to the additional coordination of the heteroatom in the chlorobenzene case or Ir−O interaction in the anisole case. The stability of both η^2-arene and η^2_{C-H} complexes in the anisole case is slightly (1−2 kcal/mol) higher than in the chlorobenzene one. However these differences are small, and in general, the stability is comparable for analogous isomers of anisole and chlorobenzene, supporting the experimental observation of slightly different ratios of their formation in the competition experiments.

Discussion

C−H Activation of Benzene. Aromatic C−H bond activation processes by late transition metals have been studied mechanistically, yielding important insights.[1] While aliphatic σ-complexes[38] have drawn great attention in view of their relevance to saturated hydrocarbon activation, aromatic η^2_{C-H} σ-bonding is less studied.[39,40] Recently, we have reported an experimental and computational DFT study of the C−H activation mechanism in both aliphatic and aromatic PC−Rh systems. C−H activation in both cases was found to take place through a η^2_{C-H} complex.[41]

In the current work, our experimental observations, supported by the theoretical studies, indicate that the overall rate-determining step in the C−H activation process by (PNP)Ir(COE)$^+PF_6^-$ (**1**) is dissociation of COE to form the T-shaped (PNP)Ir(I) 14*e* species ($\Delta G^‡ = 32$ kcal/mol for Me-PNP). The lack of kinetic isotopic effect (vide supra) in the C−H activation process indicates that the C−H cleavage occurs after the rate-determining step supporting the calculations. The formation of a 14*e* M(I) (M = Rh, Ir) species is suggested to be an important step in C−H activation processes.[24b,42−44] From the calculations we can see that this species is in fact high in energy and stabilized by coordination of the arene. Two coordination modes are found possible for benzene, η^2_{C-C} and η^2_{C-H}, the latter being an intermediate before the actual C−H cleavage step. The isomerization between the two coordination modes has the highest barrier following COE dissociation barrier (10.4 kcal/mol), while the actual C−H bond cleavage was found to be almost barrierless. Moreover, it is anticipated that the formation of the η^2_{C-C} complex **C3** is essential for the C−H activation process[1e] to occur since it brings the C−H bond into close proximity to the metal and, by that, favors η^2_{C-H} formation and lowers the barrier for the C−H activation reaction. Formation of (PNP)Ir(H)(Ph)$^+PF_6$ (**2**) was found to be a thermodynamic sink for the overall reaction. **2** is 8.8 kcal/mol more stable than (PNP)Ir(COE)$^+PF_6$ (**1**).

Complex **2** is exceptionally stable for a coordinatively unsaturated square-pyramidal iridium complex. An unsaturated, thermally stable, hydrido-aryl trigonal bipyramidal complex, Ir(P^iPr_3)$_2$(H)(Ph)(Cl), reported by Werner,[21] is stabilized by strong π-donation of the chloride ligand to an empty d-orbital of the metal. This type of stabilization is absent in **2**. Recently, Goldman reported a closely related (PCP)Ir(H)(Ph) (PCP = η^3-2,6-(tBu_2PCH_2)$_2C_6H_3$) complex.[22] Complex **2** and (PCP)Ir(H)(Ph) represent a rare case of a differently charged, isoelectronic couple of *the same metal* that undergoes C−H reductive elimination−oxidative addition. While complex **2** exhibits high thermal stability, the neutral (PCP)Ir(H)(Ph) exhibits a relatively high exchange rate with other arenes even at room temperature and is stable only at −10 °C. This seems counterintuitive, since the electron density at the metal center in the neutral PCP system is expected to be higher than in the cationic PNP system, which is expected to make the latter more prone to C−H reductive elimination. Both experiments and calculations showed that, indeed, the electron density at the metal center in the PCP system is higher. Thus, the CO stretching frequency of (PCP)Ir(H)(Ph)(CO) is 1973 cm^{-1} versus 2005 cm^{-1} of the PNP system. According to calculations, the Ir−C_{Ph} bond in the PCP system is longer than the Ir−C_{Ph} bond of the PNP system, which is attributed to the higher *trans* influence of the aryl PCP ring versus the pyridine PNP one and explains the lower stability of (PCP)Ir(H)(Ph).

The reactivity of another closely related complex, (PNP)Ir(H)(Ph) (PNP = bis(2-(diisopropylphosphino)-4-methylphenyl)amine), was recently reported by Ozerov et al.[11d] The electron density at the Ir(III) center of this neutral complex is expected to be higher than in the case of the cationic complex **2**. As in the case of **2**, Ozerov's complex did not exhibit fast arene exchange at room temperature, unlike Goldman's (PCP)Ir(H)(Ph), most probably as a result of the lower *trans* influence of the PNP (amine) ligand compared to that of the PCP (aryl).

Experimental work demonstrates that heating the C−H activation complex (PNP)Ir(Ph)(H)$^+$ at 60 °C with other arenes results in arene exchange.[17] This process can in principle take place by dissociative or associative mechanisms. Both mechanisms are expected to take place from the Ir(I) intermediates, complexes η^2_{C-C} **C3** and η^2_{C-H} **C4**, rather than from the (PNP)Ir(Ph)(H)$^+$ complex **C5**. The computational results indicate that C−H reductive elimination, leading to the η^2_{C-H} intermediate **C4**, has a relatively low barrier ($\Delta G^‡ = 11$ kcal/mol), as does the reaction **C4** → **C3** ($\Delta G^‡ = 3$ kcal/mol). A computational search for an associative exchange of benzene found one transition state for the exchange of two benzene ligands in the η^2_{C-H} configuration (**TS**−**C4**−**C4**). The barrier found for the associative exchange is ∼20 kcal/mol, which is 12 kcal/mol higher in energy than the dissociation of benzene leading to the T-shaped complex **C2**. Thus the dissociative pathway for benzene exchange is more likely to take place in this system.[45] The more bulky tBu subsituents would further favor a dissociative mechanism. Arene exchange in the similar (tBu-PCP)Ir system was suggested to take place dissociatively based on both computational DFT and experimental study.[22,46]

C−H Activation of Haloarenes and Anisole. The importance of a coordinating moiety in directing C−H activation

toward the *ortho*-position of an arene was reported for carbonyl and nitrile groups in various systems, both experimentally and theoretically. Formation of a stable metallacycle was suggested to account for the observed reactivity. Although in most cases the metallacycle obtained is a stable five- or six-membered ring complex, three- and four-membered metallacycles are also known.[47] The C−H activation process by the Ir(PNP) system can be viewed as a cyclometalation assisted by weak coordination of the halide atom or the oxygen atom (in anisole). Examples of chloro- and bromoarene coordination are not common.[27] Moreover, the coordination-assisted C−H activation of those compounds is rare. In our experimental work we have compared the activation selectivity of fluorobenzene, chlorobenzene, bromobenzene, and anisole. In general, there is a correlation between the observed kinetic selectivity, which increased upon going from fluorobenzene to bromobenzene, and the polarizability of the halogen atoms. As the polarizability increases in descending the periodic table from fluorine to bromine, the coordination ability of the halide substituent increases.

Indeed, lack of selectivity was observed experimentally in the C−H activation of fluorobenzene with complex **1**. Recently, a theoretical and experimental study on the sensitivity of the M−C bond strength to substituents was reported.[27] It was shown that the *ortho* C−H bond in fluorobenzene is the strongest C−H bond in this molecule, and thus, the M−C bond in this position is the strongest one, resulting in a thermodynamic preference for C−H activation at the *ortho*-position. Caulton showed[15b] that an Os(II) complex activates the *ortho* C−H bond preferentially in fluoroarenes. This was explained to be a result of preferential interaction of Os with the π-cloud *ortho* to the C−F bond, making the *ortho* activation kinetically favored.[15b] In our case a slight thermodynamic preference was found in favor of the *ortho*- versus the *para*-isomer and even a higher preference versus the *meta*-isomer. The kinetically nonselective activation of fluorobenzene can be explained by the low coordination ability of the fluorine substituent, and the slight thermodynamic selectivity can be attributed to bond strength.

Although chelation-assisted selective *ortho* C−H activation in aromatic systems is well documented[4,5] and mechanistically studied, examples of similar chelation-assisted processes in haloarenes are very rare.[9,13,17] The Ir(I) cationic system exhibited kinetic and thermodynamic selectivity toward the C−H bond *ortho* to the halide atom (chloro- or bromobenzene) or etheral oxygen atom (anisole). As shown experimentally and theoretically, the selectivity observed might be due to precoordination of the halogen atom or the oxygen atom to the metal center. Such precoordination, like the η^2_{C-C} arene coordination, has an accessible pathway toward C−H activation.

In general the C−H activation of chlorobenzene is essentially similar to that of benzene, although a much more complicated mechanism occurs with chlorobenzene due to the lack of symmetry and coordination through chloride. Indeed, according to both experiment and theory, there is a distribution of several possible C−H activation complexes, which were obtained kinetically (*ortho* (**C8** and **C20**), *meta* (**C13** and **C17**), and *para*-Cl (**C15**) C−H-activated complexes), but the *ortho* C−H activation complex, **C8**, is the kinetically favored one. Moreover, it is 10 kcal/mol more stable thermodynamically due to coordination of the Cl atom to the metal center and, thus, is the sole product observed in NMR after continued heating at 60 °C, as shown experimentally.

An interesting comparison can be made with the *neutral* (PNP)Ir(I) complex reported by Ozerov,[11d] where only 71% selectivity toward the *ortho*-C−H bond of chlorobenzene was observed. Indeed, no coordination of the chloride atom in the C−H activation product (PNP)Ir(H)(*o*-C_6H_4Cl) was seen. Obviously, Cl coordination to a cationic Ir(III) center is more favorable than to a neutral one. Lack of the extra stabilization gained by coordination of the chlorine atom to the metal center can explain the lower selectivity in that case.

According to calculations, arene C−H activation was found to take place directly only from η^2_{C-H} complexes, whereas the η^2-arene complexes are responsible for facilitating formation of η^2_{C-H} complexes and interchanging between different positions along the aromatic ring. However, a Cl-coordinated intermediate can be also formed in this system, which might favor the *ortho*-Cl C−H activation. Thus both η^2-arene and Cl-coordinated intermediates serve as predirecting intermediates toward the formation of certain η^2_{C-H} complexes necessary for C−H activation to occur. However, since the Cl-coordinated complex was found in the calculations to be substantially more stable than the arene η^2_{C-C} complexes, it might explain the kinetic preference of the *ortho*-Cl C−H activation complex over other C−H activation isomers, which can be obtained only from the less stable η^2_{C-C} complexes.

The C−Cl bond cleavage is not observed experimentally, although theoretically the C−Cl oxidative addition product is as stable as the activation products of the *meta* and *para* C−H bonds. According to the calculations, the reason is kinetic. Both C−H and C−Cl activation proceed from the Cl-coordinated intermediate, but the barrier to C−Cl activation is much higher, probably as a result of steric hindrance inflicted by the *tert*-butyl substituents on the phosphines. Remarkably, the normally facile oxidative addition of the Ph−Br bond to electron-rich Ir(I)[48] was not observed, although this bond is significantly weaker then C−H bonds and prone to nucleophilic attack. The selective activation of anisole is governed mostly by the same factors as in the case of chlorobenzene, with the heteroatom (oxygen of anisole) serving as a directing moiety.[49] In the case of anisole it is less obvious why the *ortho*-isomer is also thermodynamically the most stable one. Both calculations and X-ray analysis, supported by NMR, did not show significant coordination of the methoxy moiety to the metal center. Some structural clues are relevant. Comparing the Ir−C_{ipso}−C bond angle in (PNP)Ir(H)(C_6H_5) (**2**) (125.1°), (PNP)Ir(H)(C_6H_4Cl) (**8a**) (134.3°), and (PNP)Ir(H)(C_6H_4OMe) (**10a**) (131.1°), it is largest in **8a** and smallest in **2**, implying in the case of anisole an interaction of the oxygen atom with the metal center. Such an interaction could be electrostatic (δ^+ on Ir, δ^- on oxygen).

Comparison between the Different C−H Activation Processes. As observed in the exchange experiments, (PNP)Ir(H)(Ph) (**2**) underwent exchange with other arenes at lower temperature relative to complexes **8a**, **9a**, and **10a**. The lack of ligand coordination in the empty coordination site, *trans* to the hydride, contributes greatly to such reactivity. Indeed, when acetonitrile was added as the sixth ligand, the reductive elimination of benzene slowed. A more profound effect was observed when the sixth ligand was CO, in which case reductive elimination was observed only above 110 °C. C−H reductive elimination from Rh(III) and Ir(III) octahedral complexes was

(47) Ryabov, A. D. *Chem. Rev.* **1990**, *90*, 403.

(48) Yamamoto, A. *Organotransition Metal Chemistry*; John Wiley & Sons: New York, 1986.

(49) It is important to point out that the C−H_{sp3} bond was not activated under those conditions. However, at elevated temperatures C−H_{sp3} bond cleavage is observed. This is under study and will be reported in a future paper.

shown to involve ligand loss.[24] Both experiments and calculations show that coordination of the heteroatom to the metal center after the C−H activation process increases the kinetic barrier for reductive elimination and thus further stabilizes the *ortho*-activated products in comparison to (PNP)Ir(H)(Ph).

It was shown experimentally that the three different *ortho* C−H-activated complexes (PNP)Ir(H)(C_6H_4Cl), (PNP)Ir(H)-(C_6H_4Br), and (PNP)Ir(H)(C_6H_4OMe) have comparable *kinetic* stability. However, upon heating a solution of either complex (PNP)Ir(H)(C_6H_4X) at 70 °C in a solution of anisole/chlorobenzene or anisole/bromobenzene (1:1 molar ratio), arene exchange occurred. Under those conditions the *ortho*-activated anisole complex is the most stable one thermodynamically, followed by the chlorobenzene and bromobenzene *ortho*-isomers (in that order). The *para*- and *meta*-isomers under those conditions are the least stable, as they disappear after prolonged heating (70 °C for 5 days). Examining the calculated bond strengths of the *ortho*, *meta*, and *para* C−H bonds of the haloarenes and anisole, it is possible to see a correlation between the bond strength and the observed thermodynamic stability of the C−H activation product.[50] In anisole and fluorobenzene the *ortho* C−H bond is strongest (compared to the other haloarenes) and the difference in bond strength between the *meta* and *para* ones is the largest. This correlates with an even stronger M−C bond at the *ortho*-position.[15] However, while in the case of anisole kinetic as well as thermodynamic preference was observed, with fluorobenzene no kinetic effect was observed, supporting coordination-assisted C−H activation with anisole. Moreover, despite the fact that the energy difference between the arene C−H bonds is lower in chlorobenzene and bromobenzene, kinetic and thermodynamic preference was observed toward the *ortho* C−H bond.

Conclusions

An experimental and theoretical study of the C−H activation of aromatic C−H bonds by an electron-rich $(PNP)Ir(COE)^+$ complex was presented here. Activation of benzene involves a dissociative mechanism via the formation of a three-coordinate 14*e* Ir(PNP) intermediate, formation of which is the rate-determining step of the whole process. Two coordination modes are found possible for benzene, η^2_{C-C} and η^2_{C-H}, both of which are involved in the C−H activation process; the η^2_{C-C} intermediate brings the metal to the proximity of the C−H bond, followed by its isomerization to the η^2_{C-H} intermediate, which undergoes C−H cleavage. The isomerization between the two coordination modes has the highest barrier following COE dissociation barrier, while the cleavage of the C−H bond is almost barrierless.

A rare case of two isoelectronic, differently charged systems of the same metal, $(PNP)Ir(H)(Ph)^+$ and (PCP)Ir(H)(Ph), which undergo C−H oxidative addition/reductive elimination, was examined experimentally and computationally. It was illustrated both experimentally and theoretically that the cationic PNP system has a lower electron density at the metal center. A higher *trans* influence of the *ipso* carbon of the PCP system as compared with the pyridinic nitrogen is evident theoretically and explains the lower stability of the (PCP)Ir(H)(Ph) system.

Rare, selective C−H bond activation of haloarenes and anisole was also studied experimentally and theoretically. Experiments have indicated that the activation is directed by heteroatom coordination, the effect being both kinetic and thermodynamic; that is, heteroatom coordination directs the metal to the *ortho*-position and stabilizes the activation product. A lower selectivity was observed in the case of the neutral PNP complex reported by Ozerov[11d] (vide supra), where no coordination of the heteroatom to the metal center took place following C−H activation. As shown theoretically by ONIOM calculations of the t-Bu derivatives of **C6** and **C22**, after COE dissociation from complex **1** takes place, the most stable intermediates are the heteroatom-coordinated complexes of chlorobenzene and anisole. The t-Bu η^2_{C-C} analogues of **C9** and **C30**, which are similar to the η^2_{C-C} intermediate of benzene, were shown to be less stable, pointing out the importance of heteroatom coordination in directing the C−H activation. Moreover, the calculated *ortho*-activated complexes **C8** and **C27** are the most stable ones thermodynamically, with the highest barriers for reductive elimination, due to heteroatom coordination (or interaction in the anisole case).

The unobserved C−Cl activation process was shown computationally to involve the same critical Cl-coordinated intermediate, as in the C−H activation process, but it experiences a higher activation barrier, and the *ortho* C−H activation product is also thermodynamically more stable than the C−Cl oxidative addition complex. Thus, theory supports the experimentally observed selective C−H bond activation. Examples of chlorine and bromine as directing moieties are scarce[13] and may suggest new ways for selective functionalization of haloarenes by C−H activation while retaining the normally more reactive C−halogen bond.

Experimental Section

Computational Methods. All calculations were carried out using Gaussian 98 program revision A.11[51] and Gaussian 03 revision C.01[52] running on the Linux farms of Martin group and of the Faculty of Chemistry Linux farm.

The mPW1k (modified Perdew−Wang one-parameter for kinetics) exchange−correlation functional of Truhlar and co-workers[53]

(50) Calculated C−H bond strength in kcal/mol at 298 K: *ortho*-anisole 476.2, *meta*-anisole 466.8, *para*-anisole 471.9, *ortho*-bromobenzene 472.5, *meta*-bromobenzene 467.6, *para*-bromobenzene 470.6, *ortho*-chlorobenzene 473.9, *meta*-chlorobenzene 468.0, *para*-chlorobenzene 471.0, *ortho*-fluorobenzene 478.5, *meta*-fluorobenzene 468.2, *para*-fluorobenzene 471.8.

(51) Frisch, M. J.; Trucks, G. W.; Schlegel, H. B.; Scuseria, G. E.; Robb, M. A.; Cheeseman, J. R.; Zakrzewski, V. G.; Montgomery, J. A., Jr.; Stratmann, R. E.; Burant, J. C.; Dapprich, S.; Millam, J. M.; Daniels, A. D.; Kudin, K. N.; Strain, M. C.; Farkas, O.; Tomasi, J.; Barone, V.; Cossi, M.; Cammi, R.; Mennucci, B.; Pomelli, C.; Adamo, C.; Clifford, S.; Ochterski, J.; Petersson, G. A.; Ayala, P. Y.; Cui, Q.; Morokuma, K.; Salvador, P.; Dannenberg, J. J.; Malick, D. K.; Rabuck, A. D.; Raghavachari, K.; Foresman, J. B.; Cioslowski, J.; Ortiz, J. V.; Baboul, A. G.; Stefanov, B. B.; Liu, G.; Liashenko, A.; Piskorz, P.; Komaromi, I.; Gomperts, R.; Martin, R. L.; Fox, D. J.; Keith, T.; Al-Laham, M. A.; Peng, C. Y.; Nanayakkara, A.; Challacombe, M.; Gill, P. M. W.; Johnson, B.; Chen, W.; Wong, M. W.; Andres, J. L.; Gonzalez, C.; Head-Gordon, M.; Replogle, E. S.; Pople, J. A. *Gaussian 98, Revision A.11*; Gaussian, Inc.: Pittsburgh, PA, 2001.

(52) Frisch, M. J.; Trucks, G. W.; Schlegel, H. B.; Scuseria, G. E.; Robb, M. A.; Cheeseman, J. R.; Montgomery, Jr., J. A.; Vreven, T.; Kudin, K. N.; Burant, J. C.; Millam, J. M.; Iyengar, S. S.; Tomasi, J.; Barone, V.; Mennucci, B.; Cossi, M.; Scalmani, G.; Rega, N.; Petersson, G. A.; Nakatsuji, H.; Hada, M.; Ehara, M.; Toyota, K.; Fukuda, R.; Hasegawa, J.; Ishida, M.; Nakajima, T.; Honda, Y.; Kitao, O.; Nakai, H.; Klene, M.; Li, X.; Knox, J. E.; Hratchian, H. P.; Cross, J. B.; Bakken, V.; Adamo, C.; Jaramillo, J.; Gomperts, R.; Stratmann, R. E.; Yazyev, O.; Austin, A. J.; Cammi, R.; Pomelli, C.; Ochterski, J. W.; Ayala, P. Y.; Morokuma, K.; Voth, G. A.; Salvador, P.; Dannenberg, J. J.; Zakrzewski, V. G.; Dapprich, S.; Daniels, A. D.; Strain, M. C.; Farkas, O.; Malick, D. K.; Rabuck, A. D.; Raghavachari, K.; Foresman, J. B.; Ortiz, J. V.; Cui, Q.; Baboul, A. G.; Clifford, S.; Cioslowski, J.; Stefanov, B. B.; Liu, G.; Liashenko, A.; Piskorz, P.; Komaromi, I.; Martin, R. L.; Fox, D. J.; Keith, T.; Al-Laham, M. A.; Peng, C. Y.; Nanayakkara, A.; Challacombe, M.; Gill, P. M. W.; Johnson, B.; Chen, W.; Wong, M. W.; Gonzalez, C.; and Pople, J. A. *Gaussian 03, Revision C.02*; Gaussian, Inc.: Wallingford, CT, 2004.

(53) Lynch, B. J.; Fast, P. L.; Harris, M.; Truhlar, D. G. *J. Phys. Chem. A* **2000**, *104*, 4811

was employed in conjunction with the SDD and SDB-cc-pVDZ basis sets (see below). The mPW1k functional was previously shown[54,55] to typically yield more reliable reaction barrier heights than other exchange−correlation functionals.

The SDD basis set is the combination of the Huzinaga−Dunning double-ζ basis set on lighter elements with the Stuttgart−Dresden basis set−relativistic effective core potential (RECP) combination[56] on the transition metals. The SDB-cc-pVDZ basis set combines the Dunning cc-pVDZ basis set[57] on the main group elements with the Stuttgart−Dresden basis set−RECP combination[56] on the transition metals, with an f-type polarization exponent taken as the geometric average of the two f-exponents given in the Appendix to ref 58.

The energetics for our final reaction profiles obtained from the mPW1k functional with the SDD basis set were validated by single-point energy calculations, using the SDD reference geometries, with the extended SDB-cc-pVDZ basis set.

For tBu-PNP, two-layer ONIOM[59] approach was employed, in which the *tert*-butyl groups on the phosphorus were placed in the outer layer and the remainder of the system was placed in the inner layer. For technical reasons, the mPW1k functional was used for both layers. In the anisol case, an additional ONIOM calculation was performed with the Becke97-1 (B97-1) functional,[60] as it has been shown that in some instances this functional is more suitable for determining molecular equilibrium properties.[61] Both in mPW1k and in B97-1 functionals, for the inner layer the valence Los Alamos National Laboratory double-ζ (LANL2DZ) basis set−RECP combination was used,[62] while for the outer layer, the LANL1MB basis set−RECP combination was employed.[62] (As is customary, first-row atoms in this approach were treated by means of the Dunning−Hay valence double-ζ[63] basis set.) The energetics for our final tBu-PCP geometries were validated by single-point energy calculations, using the ONIOM(mPW1k/LANL2DZ:mPW1k/LANL1MB) or ONIOM(B97-1/LANL2DZ:B97-1/LANL1MB) reference geometries, and at the higher level of theory mPW1k/LANL2DZ+P or B97-1/LANL2DZ+P, respectively, where the "+P" stands for the addition of polarization functions with exponents taken from ref 64.

Geometry optimizations for minima were carried out using the standard Schlegel algorithm[65] in redundant internal coordinates until in the neighborhood of the solution and then continued using analytical second derivatives.[66] Optimizations for transition states were carried out with an initial guess for the transition state being generated from manual manipulation of the geometry using MOLDEN.[67] In cases where this approach failed to converge, we used analytical second derivatives at every step.

Zero-point and RRHO (rigid rotor harmonic oscillator) thermal corrections (to obtain ΔS and ΔG values) were obtained from the unscaled computed frequencies.

Where necessary, the Grid = UltraFine combination, i.e., a pruned (99 590) grid in the integration and gradient steps and a pruned (50 194) grid in the CPKS (coupled perturbed Kohn−Sham) steps, was used as recommended in ref 68.

For interpretative purposes, atomic partial charges and Wiberg bond indices[69] were obtained by means of a natural population analysis (NPA)[70] at the mPW1k/LANL2DZ level for the tBu-PCP complexes.

Experimental Methods. General Procedures. All experiments with metal complexes and phosphine ligands were carried out under an atmosphere of purified nitrogen in a Vacuum Atmospheres glovebox equipped with a MO 40-2 inert gas purifier or using standard Schlenk techniques. All solvents were reagent grade or better. All nondeuterated solvents were refluxed over sodium/benzophenone ketyl and distilled under argon atmosphere. Deuterated solvents were used as received. All the solvents were degassed with argon and kept in the glovebox over 4 Å molecular sieves. Commercially available reagents were used as received.

^{1}H, ^{13}C, ^{31}P, and ^{19}F NMR spectra were recorded at 400, 100, 162, and 376 MHz, respectively, using a Bruker AMX-400 NMR spectrometer. All spectra were recorded at 23 °C. ^{1}H NMR and ^{13}C{^{1}H} NMR chemical shifts are reported in ppm downfield from tetramethylsilane. ^{1}H NMR chemical shifts were referenced to the residual hydrogen signal of the deuterated solvents (3.58 ppm, tetrahydrofuran; 5.32 ppm, dichloromethane). In ^{13}C{^{1}H} NMR measurements the signals of THF-d_8 (67.5 ppm) and CD_2Cl_2 (53.8 ppm) were used as a reference. ^{31}P NMR chemical shifts are reported in parts per million downfield from H_3PO_4 and referenced to an external 85% solution of phosphoric acid in D_2O. ^{19}F NMR chemical shifts were referenced to C_6F_6 (−163 ppm). Screw-cap 5 mm NMR tubes were used in the NMR follow-up experiments. Abbreviations used in the description of NMR data are as follows: br, broad; s, singlet; d, doublet; t, triplet; q, quartet; m, multiplet; v, virtual.

Reaction of [Ir(COE)$_2$(acetone)$_2$][PF$_6$] with PNP (PNP = 2,6-Bis(di-tBu-phosphinomethylene)pyridine; COE = cyclooctene). Preparation of [Ir(PNP)(COE)][PF$_6$] (1). An acetone solution (2 mL) of PNP (50 mg, 0.126 mmol) was added dropwise to an acetone solution (2 mL) of [Ir(COE)$_2$(acetone)$_2$][PF$_6$][18] (85.2 mg, 0.126 mmol). Upon addition of PNP, the color turned dark purple-red. The mixture was stirred for an additional 2 min at room temperature, then poured into pentane, causing precipitation of complex **1** as a pink-red solid. The solid was separated by decantation and dried under vacuum, resulting in a quantitative yield of complex **1**.

[Ir(PNP)(COE)][BAr^F]. To an acetone suspension (5 mL) of [Ir(COE)$_2$-μ-Cl]$_2$ (200 mg, 0.223 mmol) were added 3 equiv of NaBAr^F (592 mg, 0.670 mmol). The slurry was stirred for 4 h at room temperature until the color changed to red-purple. The solution was filtered through Celite, the solvent was evaporated, and the residue was washed with pentane (15 mL) and then washed with ether. The pinkish solid was left under vacuum for one night, resulting in 80% yield. ^{31}P{^{1}H} NMR (acetone-d_6): 44.00 (d, J_{pp} = 318.0 Hz, *P*-Ir-P), 49.00 (d, J_{pp} = 318.0 Hz, P-Ir-*P*), −150.00 (heptet, J_{FP} = 713.0 Hz, PF_6). ^{1}H NMR (acetone-d_6): 1.47 (dd,

(54) (a) Parthiban, S.; de Oliveira, G.; Martin, J. M. L. *J. Phys. Chem. A* **2001**, *105*, 895. (b) Lynch, B. J.; Truhlar, D. G. *J. Phys. Chem. A* **2001**, *105*, 2936.

(55) Iron, M. A.; Lo, H. C.; Martin, J. M. L.; Keinan, E. *J. Am. Chem. Soc.* **2002**, *124*, 7041.

(56) Dolg, M. In *Modern Methods and Algorithms of Quantum Chemistry*; Grotendorst, J., Ed.; John von Neumann Institute for Computing: Jülich, 2000; Vol. 1, p 479.

(57) Dunning, T. H., Jr. *J. Chem. Phys.* **1989**, *90*, 1007.

(58) Martin, J. M. L.; Sundermann, A. *J. Chem. Phys.* **2001**, *114*, 3408.

(59) Dapprich, S.; Komaromi, I.; Byun, K. S.; Morokuma, K.; Frisch, M. J. *J. Mol. Struct.* (*THEOCHEM*) **1999**, *461*, 1, and references therein.

(60) Hamprecht, F. A.; Cohen, A. J.; Tozer, D. J.; Handy, N. C. *J. Chem. Phys.* **1998**, *109*, 6264.

(61) Boese, A. D.; Martin, J. M. L.; Handy, N. C. *J. Chem. Phys.* **2003**, *119*, 3005.

(62) Hay, P. J.; Wadt, W. R. *J. Chem. Phys.* **1985**, *82*, 270.

(63) Dunning, T. H.; Hay, P. J. In *Modern Theoretical Chemistry*; Schaefer, H. F., III, Ed.; Plenum: New York, 1976; Vol. 3.

(64) (a) Hollwarth, A.; Bohme, M.; Dapprich, S.; Ehlers, A. W.; Gobbi, A.; Jonas, V.; Kohler, K. F.; Stegmann, R.; Veldkamp, A.; Frenking, G. *Chem. Phys. Lett.* **1993**, *208*, 237. (b) Ehlers, A. W.; Bohme, M.; Dapprich, S.; Gobbi, A.; Hollwarth, A.; Jonas, V.; Kohler, K. F.; Stegmann, R.; Veldkamp, A.; Frenking, G. *Chem. Phys. Lett.* **1993**, *208*, 111.

(65) (a) Schlegel, H. B. *J. Comput. Chem.* **1982**, *3*, 214. (b) Peng, C.; Ayala, P. Y.; Schlegel, H. B.; Frisch, M. J. *J. Comput. Chem.* **1996**, *17*, 49.

(66) Stratmann R. E.; Burant J. C.; Scuseria G. E.; Frisch M. J. *J. Chem. Phys.* **1997**, *106*, 10175.

(67) Schaftenaar, G. *Molden 3.6*, 1999. URL: http://www.cmbi.kun.nl/~schaft/molden/molden.html.

(68) Martin, J. M. L.; Bauschlicher, C. W.; Ricca, A. *Comput. Phys. Commun.* **2001**, *133*, 189.

(69) Wiberg, K. B. *Tetrahedron* **1968**, *24*, 1083.

(70) Reed, A. E.; Curtiss, L. A.; Weinhold, F. *Chem. Rev.* **1988**, *88*, 899.

$^5J_{PH}$ = 1.8 Hz, $^3J_{PH}$ = 3.8 Hz), 1.42 (dd, $^5J_{PH}$ = 2.0 Hz, $^3J_{PH}$ = 4.3 Hz, 18H, P-C(CH_3)$_3$), 1.44−1.50 (m, 10H, aliphatic hydrogens of COE), 2.55 (m, 2H, CH_2-CH═CH), 4.07 (vt, J_{PH} = 7.9 Hz, 4H, CH_2-P), 4.20 (m, 2H vinylic hydrogens of COE), 7.87 (d, $^3J_{HH}$ = 7.8 Hz, 1H, PNP-aryl-H), 7.97 (d, $^3J_{HH}$ = 7.6 Hz, 1H, PNP-aryl H), 8.25 (t, $^3J_{HH}$ = 7.7 Hz, 1H, PNP-aryl H). ^{19}F NMR (acetone-d_6): −73 (d, $^1J_{PF}$ = 713.0 Hz, PF_6). ^{13}C{^{1}H} NMR (acetone-d_6): 30.6 (m, PC(CH_3)$_3$), 36.2−36.5 (m, CH_2P), 54 (s, 2H, CH═CH), 120 (dd, $^3J_{PC}$ = 7.4 Hz, $^5J_{PC}$ = 10.1 Hz, PNP-aryl C), 141.6 (s, PNP-aryl C), 164.3 (d, $^2J_{PC}$ = 13.0 Hz, PNP aryl-C). [BAr^F] signals: ^{1}H NMR (acetone-d_6) 7.7 (s, 8H), 8.0 (s, 4H); ^{19}F NMR (acetone-d_6) −60 (s). Assignment of the signals was confirmed by DEPT. Anal. Calcd for **1** (counteranion PF_6^-), $C_{31}H_{57}P_3F_6NIr$: C, 44.17; H, 6.82. Found: C, 44.25; H, 6.76.

Reaction of [Ir(PNP)(COE)][PF$_6$] (1) with Benzene. Formation of [Ir(PNP)(H)(Ph)][PF$_6$] (2). A solution (3 mL) of complex **1** (15 mg, 0.039 mmol) in benzene was heated at 60 °C for 1 h, during which the color changed to orange. The solvent was evaporated and the orange solid was washed with pentane and dried under vacuum overnight, resulting in pure complex **2** in quantitative yield. Compound **2** was obtained also by dissolving complex **1** in benzene and leaving it for 4 days at room temperature. ^{31}P{^{1}H} NMR (hydride coupled, CD_2Cl_2): 54.00 (d, $^2J_{HP}$ = 10.0 Hz), −150.0 (heptet, $^1J_{FP}$ = 713 Hz, PF_6). ^{1}H NMR (CD_2Cl_2): −43.9 (vt, $^2J_{PH}$ = 12 Hz, 1H, *H*-Ir), 1.18 (dd, $^5J_{PH}$ = 6.9 Hz, $^3J_{PH}$ = 14.2 Hz, 18H, P-C(CH_3)$_3$), 3.90 (m, 4H, CH_2-P), 6.80 (t, $^2J_{HH}$ = 7.3 Hz, 1H, aryl-*H*), 6.93 (t, $^2J_{HH}$ = 6.2 Hz, 1H, aryl-*H*), 7.06 (t, $^2J_{HH}$ = 7.3 Hz, 1H, aryl-*H*), 7.32 (d, J_{HH} = 7.6 Hz 2H, aryl-*H*), 7.7 (d, J_{HH} = 7.8 Hz, 2H, *H*-PNP-aryl), 7.96 (t, J_{HH} = 7.8 Hz, 1H, *H*-PNP-aryl). Assignment of signals was confirmed by COSY. NOE effect was observed between hydride at −43.9 ppm and protons at 7.32 ppm. ^{13}C{^{1}H} NMR (CD_2Cl_2): 27.9−29.6 (m, P-C(CH_3)$_3$), 36 (m, CH_2P), 122.4 (m, PNP-aryl C3,5), 126.1−136.4 (singlets, phenyl carbons), 139.6 (s, PNP-aryl, C4), 145 (br t, C_{ipso}), 163.9 (s, PNP-aryl, C2,6). Assignment of the signals was confirmed by DEPT. Anal. Calcd for $C_{29}H_{49}P_3F_6NIr$: C, 42.96; H, 6.09. Found: C, 44.93; H, 6.69.

Reaction of [Ir(PNP)(COE)][PF$_6$] (1) with *m*-Xylene. Formation of [Ir(PNP)(H)(*m*-xylyl)][PF$_6$] (3). A solution (3 mL) of [Ir(PNP)(COE)][PF_6] (**1**) (15 mg, 0.039 mmol) in *m*-xylene was heated at 60 °C for 1 h, during which an orange precipitate of [Ir(PNP)(H)(*m*-xylyl)][PF_6] (**3**) was formed in quantitative yield. The solid was washed with pentane and with ether followed by high-vacuum-drying for one night. ^{31}P{^{1}H} NMR of the CD_2Cl_2 solution of **3** revealed one product. ^{31}P{^{1}H} NMR (CD_2Cl_2): 53.7 (br s), −150.0 (heptet, $^1J_{FP}$ = 713 Hz, PF_6). ^{1}H NMR (CD_2Cl_2): −43.3 (vt, $^2J_{PH}$ = 12 Hz, 1H, *H*-Ir), 1.2 (m, P-C(CH_3)$_3$, 36H), 2.4 (s, 6H, aryl-CH_3), 3.84 (m, 4H, CH_2-P), 6.43 (s, aryl-*H*), 6.90 (br s, aryl-*H*), 6.95 (br s, aryl-*H*), 7.67 (d, J_{HH} = 7.8 Hz, 2H, *H*-PNP-aryl), 7.94 (t, J_{HH} = 7.8 Hz, 1H, *H*-PNP-aryl). Assignment of signals was confirmed by COSY. ^{13}C{^{1}H} NMR (CD_2Cl_2): 21 (s, *m*-xylyl-CH_3), 21.5 (s, *m*-xylyl-CH_3), 28−30 (m, P-C(CH_3)$_3$), 37 (vt, $^1J_{PC}$ = 9.3 Hz, P-C(CH$_3$)$_3$), 38 (vt, $^1J_{PC}$ = 9.3 Hz, P-C(CH$_3$)$_3$), 39 (vt, $^1J_{PC}$ = 11.1 Hz, CH_2P), 122.4 (m, PNP-aryl C3,5), 125.1−135.3 (singlets, phenyl carbons), 139.6 (s, PNP-aryl, C4), 137 (br t, C_{ipso}), 163.9 (s, PNP-aryl, C2,6). Assignment of signals was confirmed by DEPT. Anal. Calcd for $C_{31}H_{53}P_3F_6NIr$: C, 44.38; H, 6.37. Found: C, 44.45; H, 6.31.

Synthesis of Ir(PNP)(D)(C$_6$D$_5$)][PF$_6$] (2a). Complex **2a** was synthesized in two different routs: (a) A solution (2 mL) of complex **1** (15 mg, 0.039 mmol) in C_6D_6 was heated at 60 °C for 1 h, during which the color changed to orange. The solvent was evaporated and the orange solid was washed with pentane and dried under vacuum overnight, resulting in pure complex **2a** in quantitative yield. The ^{31}P NMR spectrum revealed a signal at 54 ppm. ^{2}H NMR revealed a pattern similar to that for complex **2**. (b) The second route is by an exchange reaction. A solution of complex **2** in C_6D_6 was heated at 50 °C for 4 h, after which the ^{31}P NMR spectrum did not change and the signals of the hydride ligand and the aromatic protons in the ^{1}H NMR spectrum disappeared while appearing in the ^{2}H NMR spectrum. Leaving a solution of complex **2** in C_6D_6 at room temperature for 4 days resulted in a small exchange only.

Reaction of [Ir(PNP)(COE)][PF$_6$] (1) with CO. Formation of [Ir(PNP)(CO)][PF$_6$] (5). Into an acetone solution (3 mL) of complex **1** (15 mg, 0.039 mmol) was bubbled CO in small excess for 1 min, during which time the color changed to yellow. The solvent was evaporated and the yellow solid was washed with pentane and dried under vacuum overnight, resulting in pure complex **5** in quantitative yield. Slow evaporation of the acetone solution resulted in formation of yellow crystals suitable for X-ray analysis. ^{31}P{^{1}H} NMR (CD_2Cl_2): 75.00 (s), −150.0 (heptet, $^1J_{FP}$ = 713 Hz, PF_6). ^{1}H NMR (CD_2Cl_2): 1.15 (t, $^3J_{PH}$ = 14.2 Hz, 36H, P-C(CH_3)$_3$), 3.93 (m, 4H, CH_2-P), 7.72 (d, J_{HH} = 7.6 Hz, 2H, *H*-PNP-aryl), 8.0 (d, J_{HH} = 7.8 Hz, 2H, *H*-PNP-aryl). ^{13}C{^{1}H} NMR (CD_2Cl_2): 27.9−29.2 (m, P-C(CH_3)$_3$), 35.6 (t, $^1J_{PC}$ = 12.4 Hz, CH_2P), 122.4 (m, PNP-aryl, C3,5), 139.6 (s, PNP-aryl, C4), 166.9 (br t, PNP-aryl, C2,6), 182 (br t, Ir-CO). Anal. Calcd for $C_{24}H_{43}P_3F_6NOIr$: C, 37.89; H, 5.70. Found: C, 37.80; H, 5.76.

Reaction of [Ir(PNP)(H)(Ph)][PF$_6$] (2) with CH$_3$CN. Formation of [Ir(PNP)(H)(Ph)(CH$_3$CN)][PF$_6$] (6). To a CH_2Cl_2 solution (3 mL) of complex **2** (15 mg, 0.039 mmol) was added 1 equiv of acetonitrile, resulting in a color change to pale orange. The solvent was evaporated and the orange solid was washed with ether and dried under vacuum overnight, resulting in pure complex **6** in quantitative yield. Slow diffusion of pentane into a THF solution of complex **6** allowed formation of orange crystals suitable for X-ray analysis. ^{31}P{^{1}H} NMR (CD_2Cl_2): 37.97 (br s), −150.0 (heptet, $^1J_{FP}$ = 713 Hz, PF_6). ^{1}H NMR (CD_2Cl_2): −19.83 (br t, 1H, *H*-Ir), 1.18 (m, 36H, P-C(CH_3)$_3$), 3.73 (m, 4H, CH_2-P), 6.76 (br t, $^2J_{HH}$ = 7.3 Hz, 1H, *H*-aryl), 6.85 (br t, 2H, *H*-aryl), 7.67 (d, $^2J_{HH}$ = 7.0 Hz, 2H, *H*-aryl), 7.5 (d, J_{HH} = 8.0 Hz, 2H, *H*-PNP-aryl), 7.78 (t, J_{HH} = 7.5 Hz, 1H, *H*-PNP-aryl). ^{13}C{^{1}H} NMR (CD_2Cl_2): 4 (s, CH_3CN) 28.5−30.1 (m, P-C(CH_3)$_3$), 36.9 (vt,$^1J_{PC}$ = 9.3 Hz P-C(CH$_3$)$_3$), 38.1 (vt $^1J_{PC}$ = 9.3 Hz, P-C(CH$_3$)$_3$), 39.5 (vt,$^1J_{PC}$ =11.0 Hz, P-C(CH$_3$)$_3$), 122.4 (m, PNP-aryl C3,5), 125.3−135.6 (singlets, phenyl carbons), 139.6 (s, PNP-aryl, C4), 125 (br t, C_{ipso}), 163.9 (s, PNP-aryl, C2,6).

Reaction of [Ir(PNP)(H)(Ph)][PF$_6$] (2) with CO. Formation of [Ir(PNP)(H)(Ph)(CO)][PF$_6$] (4). Into an acetone solution (3 mL) of complex **2** (15 mg, 0.039 mmol) was bubbled a small excess of CO for 1 min, during which the color changed to pale yellow. The solvent was evaporated and the pale yellow solid was washed with pentane and dried under vacuum overnight, resulting in pure complex **4** in quantitative yield. ^{31}P{^{1}H} NMR (CD_2Cl_2): 39 (s), −150.0 (heptet, $^1J_{FP}$ = 713 Hz, PF_6). ^{1}H NMR (CD_2Cl_2): −7.6 (t, $^2J_{PH}$ = 12 Hz, 2H, *H*-Ir), 1.19 (m, P-C(CH_3)$_3$, 36H), 3.8 (m, 4H, CH_2-P), 6.85 (br t, $^2J_{HH}$ = 7.3 Hz, 2H, *H*-aryl), 6.91 (br t, 2H, *H*-aryl,), 7.67 (d, $^2J_{HH}$ = 7.0 Hz, 1H, *H*-aryl), 7.5 (d, J_{HH} = 8.0 Hz, 2H, *H*-PNP-aryl), 7.78 (t, J_{HH} = 7.5 Hz, 1H, *H*-PNP-aryl). ^{13}C{^{1}H} NMR (CD_2Cl_2): 29.5−31.1 (m, P-C(CH_3)$_3$), 37.9 (vt,$^1J_{PC}$ = 9.3 Hz, P-C(CH$_3$)$_3$), 39.1 (vt $^1J_{PC}$ = 9.3 Hz, P-C(CH$_3$)$_3$), 41.5 (vt,$^1J_{PC}$ = 11.0 Hz, P-C(CH$_3$)$_3$), 122.4 (m, PNP-aryl C3,5), 125.0−135.8 (singlets, phenyl carbons), 139.6 (s, PNP-aryl, C4), 150 (br t, C_{ipso}), 164.9 (s, PNP-aryl, C2,6), 186 (br t, Ir-CO). Anal. Calcd for $C_{30}H_{49}P_3F_6NOIr$: C, 42.95; H, 5.85. Found: C, 42.81; H, 6.05.

Reaction of [Ir(PNP)(H)(Ph)(CO)][PF$_6$] (4) with Anisole. When complex **4** (15 mg, 0.0178 mmol) was heated in anisole at 80 °C for 72 h, no reaction took place. Upon heating complex **4** in anisole at 110 °C for 48 h, elimination of benzene occurred, forming complex **5** in quantitative yield. The same reaction was repeated in DMSO with the same results.

Reaction of [Ir(PNP)(H)(Ph)(CH$_3$CN)][PF$_6$] (6) with Benzene-d_6. Heating a solution of **6** (15 mg, 0.0176 mmol) in benzene-d_6 at 70 °C for 48 h resulted in no obsevable reaction. However, heating

at 85 °C for the same period of time resulted in an exchange reaction. The hydride and aromatic signals disappeared and the corresponding ^{2}H signals appeared in ^{2}H NMR.

Reaction of [Ir(PNP)(COE)][PF6] (1) with Benzene-h_6/Benzene-d_6. Determination of the Kinetic Isotopic Effect. A solution (2 mL) of [Ir(PNP)(COE)][PF6] (**1**) (15 mg, 0.039 mmol) in benzene-h_6/benzene-d_6 mixture in a molar ratio 1:1 was left at room temperature (25 °C) for 48 h. The solution was evaporated and redissolved in CD_2Cl_2. ^{1}H NMR was measured with a delay of 25 s to ensure full spin relaxation. Two experiments were conducted: one was done without the use of internal standard where the calibration was performed relative to the benzylic protons of the PNP ligand and the second was performed using TMS as internal standard. Both experiments resulted in a 1:1 ratio of the deuterio and protio complexes, indicating no kinetic isotope effect.

Reaction of [Ir(PNP)(COE)][PF_6] (1) with Fluorobenzene. Formation of [Ir(PNP)(H)(C_6H_4F)][PF_6] (7). A solution (2 mL) of [Ir(PNP)(COE)][PF_6] (1) (15 mg, 0.039 mmol) in fluorobenzene was heated at 50 °C overnight, after which the solvent was evaporated and the solid was washed with ether. ^{31}P NMR of this solid revealed the formation of *o*-, *m*-, and *p*-C−H-activated complexes **7a**,**b**,**c**, giving rise to singlets at 55.2, 58, and 52.3 ppm, in a ratio of approximately 2:2:1, respectively. Further heating at 50 °C for 48 h resulted in a mixture of **7a** and **7c** in a ratio 1.8:1, respectively. Prolonged heating at 80 °C for another 48 h resulted in a slightly different mixture of the two isomers (2.3:1). For easier assignment of signals to the corresponding isomers, first the mixture of two isomers was characterized (*ortho* and *para*) using NOE and H-COSY. ^{31}P{^{1}H} NMR (CD_2Cl_2) **7a**: 55.2 (br d, $^2J_{HP}$ = 11.8 Hz, H-Ir-*P*-C(CH_3)$_3$), **7b**: 58.0 (br d, $^2J_{HP}$ = 10.3 Hz, H-Ir-*P*-C(CH_3)$_3$), **7c**: 52.3 (br). ^{1}H NMR (800 MHz, CD_2Cl_2) **7a**: −41.00 (br t, $^2J_{HP}$ = 11.5 Hz, *H*-Ir-P), 1.18 (m, 36H, PC(C*H*$_3$)$_3$), 3.50−3.90 (m, 4H, C*H*$_2$P), 6.70 (dt, $^3J_{HH}$ = 8.0 Hz, $^4J_{HH}$ = 1 Hz, 1H, aryl-*H*), 6.85 (br t, $^1J_{HH}$ = 8.0 Hz, 1H, aryl-*H*), 7.10 (dd, $^3J_{HH}$ = 7.0 Hz, $^4J_{HH}$ = 1.0 Hz, 1H, aryl-*H*), 7.30 (d, $^3J_{HH}$ = 7.0 Hz, 1H, aryl-*H*), 7.66 (d, $^3J_{HH}$ = 8.0 Hz, 2H, PNP-aryl *H*), 7.95 (t, $^3J_{HH}$ = 8.0 Hz, 1H, PNP-aryl *H*). NOE effect was observed between the hydride at −41.0 ppm and the proton at 7.10 ppm. 7b: −45.00 (br t, $^2J_{HP}$ = 10.0 Hz), 1.18 (m, 36H, P-C(C*H*$_3$)$_3$), 3.50−3.90 (m, 4H, C*H*$_2$P), 6.9 (m, 1H, aryl-*H*), 7.05 (m, 1H, aryl-*H*), 7.25 (t, $^3J_{HH}$ = 7.0 Hz, 1H, aryl-*H*), 7.35 (br s, 1H, aryl-*H*), 7.7 (d, $^3J_{HH}$ = 8.0 Hz, 2H, PNP-aryl), 8.00 (t, $^3J_{HH}$ = 8.0 Hz, 1H, PNP-aryl). 7c: −42.5 (br, 1H), 1.18 (m, 36H, P-C(C*H*$_3$)$_3$), 3.50−3.90 (m, 4H, C*H*$_2$P), 7.25 (d, $^3J_{HH}$ = 7.0 Hz, 1H, aryl-*H*), 7.43 (d, $^3J_{HH}$ = 7.0 Hz, 1H, aryl-*H*), 7.5 (d, $^3J_{HH}$ = 8.0 Hz, 2H, *H*-PNP-aryl), 7.90 (t, $^3J_{HH}$ = 8.0 Hz, 1H, PNP-aryl). Assignment of the signals was done by COSY. NOE effect was observed between the hydride at −42.5 ppm and protons at 7.25 ppm. Anal. Calcd for 7, $C_{29}H_{48}P_3F_7NIr$: C, 42.02; H, 5.84. Found: C, 42.09; H, 5.81.

Reaction of [Ir(PNP)(COE)][PF_6] (1) with Chlorobenzene. Formation of [Ir(PNP)(H)(C_6H_4Cl)][PF_6] (8). A solution of [Ir(PNP)(COE)][PF_6] (**1**) (15 mg, 0.039 mmol) in chlorobenzene (2 mL) was heated at 60 °C for 3 h. The solvent was evaporated, and the resulting orange solid was washed consecutively with pentane and ether, resulting in complex **8a** in quantitative yield. Monitoring the reaction by ^{31}P NMR at 50 °C revealed after 12 min 10% conversion of **1**, resulting in a ratio **8a**:**8b**:**8c** of 4:2:1. Continued heating of complex **1** for 1 h at 50 °C resulted in formation of a mixture containing 60% of the *ortho*-activated chlorobenzene **8a**, 30% of the *meta* **8b**, and 10% of the *para*-activated one **8c**. Further heating of this mixture for 48 h resulted in a sole product, the *ortho*-activated chlorobenzene complex **8a**.

Complex 8a. ^{31}P NMR (hydride coupled, CD_2Cl_2): 52.00 (d, $^2J_{PH}$ = 13.0 Hz). ^{1}H NMR (CD_2Cl_2): −34.00 (t, $^2J_{HP}$ = 13.8 Hz, 1H, *H*-Ir-P), 1.2 (m, 36H, P-C(C*H*$_3$)$_3$), 3.2−3.8 (m, 4H, C*H*$_2$P), 6.65 (dd, $^3J_{HH}$ = 8.0 Hz, $^4J_{HH}$ = 2.0 Hz, 1H, aryl-*H*), 6.91 (br t, J_{HH} = 8.0 Hz, 1H, aryl-*H*), 7.04 (dt, $^3J_{HH}$ = 7.0 Hz, $^4J_{HH}$ = 1.0 Hz,1H, aryl-*H*), 7.3 (d, $^3J_{HH}$ = 7.0 Hz, 1H, aryl-*H*), 7.58 (d, $^3J_{HH}$ = 6.6 Hz, 2H, *H*-PNP-aryl), 7.92 (t, $^3J_{HH}$ = 6.6 Hz, 1H, *H*-PNP-aryl). ^{13}C{^{1}H} NMR (400 MHz, $CDCl_3$): 28.8−29.6 (m, P-C(*C*H$_3$)$_3$), 37.1−38.7 (m, *C*H$_2$P), 121.9−142.0 (singlets, PNP-aryl C3,5; C4 and phenyl), 163.5 (d, $^2J_{PC}$ = 12.0 Hz, PNP-aryl C2,6), 163.3 (bs, C_{ipso}). NOE was observed between the hydride at −34 ppm and the proton at 6.65 ppm. Selected ^{1}H NMR data: **8b**: −41 (br s, *H*-Ir, 1H), 7.1 (m, 1H, aryl-*H*), 7.35 (m, 2H, aryl-*H*), 7.5 (m, 1H, aryl-*H*). 7.58 (d, $^3J_{HH}$ = 6.6 Hz, 2H, *H*-PNP-aryl), 7.92 (t, $^3J_{HH}$ = 6.6 Hz, 1H, *H*-PNP-aryl). NOE effect was observed between the hydride at −41 ppm and the protons at 7.35 ppm. **8c**: −44 (br s, 1H, *H*-Ir), 7.0 (d, $^3J_{HH}$ = 6.0 Hz, 2H, aryl-*H*), 7.45 (d, $^3J_{HH}$ = 6.0 Hz, 2H, aryl-*H*), 7.58 (d, $^3J_{HH}$ = 6.6 Hz, 2H, *H*-PNP-aryl), 7.92 (t, $^3J_{HH}$ = 6.6 Hz, lH, *H*-PNP-aryl). NOE was observed between the hydride at −44 ppm and the proton at 7.45 ppm. ^{31}P NMR (hydride coupled, CD_2Cl_2): **8c**,**8b**: 53−53.5 (m, *P*-Ir-*P*). Anal. Calcd for **8**, $C_{29}H_{48}P_3F_6NClIr$: C, 41.21; H, 5.72. Found: C, 41.31; H, 5.63.

Reaction of [Ir(PNP)(COE)][PF_6] (1) with Bromobenzene. Formation of [Ir(PNP)(H)(C_6H_5Br)][PF_6] (9). Complex **9** was prepared analogously to complex **8**. The *ortho*-activated bromobenzene complex **9a** amounted to 70% of the mixture upon disappearance of the starting complex **1** and the sole product after continued heating at 60 °C for 3 h or longer.

Complex 9a. ^{31}P NMR (hydride coupled, CD_2Cl_2): 49.0 (d, $^2J_{PH}$ = 11.0 Hz). ^{1}H NMR (CD_2Cl_2): −29 (t, $^2J_{PH}$ = 11.0 Hz, 1H, *H*-Ir-P), 1.25 (vt, $^3J_{PH}$ = 7.0 Hz, 18H, C(C*H* $_3$)$_3$P), 1.29 (vt, $^3J_{PH}$ = 7.0 Hz, 18H, C(C*H*$_3$)$_3$P), 3.6−3.95 (m, 4H, C*H*$_2$P), 6.73 (dd, $^3J_{HH}$ = 8.0 Hz, 1H, $^4J_{HH}$ = 1.0 Hz, *H*-aryl), 6.87 (br t, $^3J_{HH}$ = 8.0 Hz, 1H, $^4J_{HH}$ = 1.0 Hz, *H*-aryl), 7.09 (dt, $^3J_{HH}$ = 7.0 Hz, 1H, *H*-aryl), 7.25 (br d, $^3J_{HH}$ = 7.0 Hz, 1H, *H*-aryl), 7.58 (d, $^3J_{HH}$ = 8.0 Hz, 2H, *H*-PNP-aryl), 7.9 (t, $^3J_{HH}$ = 8.0 Hz, 1H, *H*-PNP-aryl). ^{13}C{^{1}H} NMR (CD_2Cl_2): 28.8−29.6 (m, P-C(*C*H$_3$)$_3$), 37−38.5 (m, *C*H$_2$P), 120−142.3 (singlets, PNP-aryl C3,5; C4 and aryl), 164 (d, $^2J_{PC}$ = 12 Hz, PNP-aryl C2,6), 163.5 (br s, C_{ipso}). NOE was observed between the hydride at −29 ppm and the proton at 7.25 ppm. Selected NMR data for **9c**: ^{1}H NMR (CD_2Cl_2): −45 (br s, *H*-Ir, 1H), 7.27 (d, $^3J_{HH}$ = 5.0 Hz, aryl-*H*, 2H), 7.52 (d, $^3J_{HH}$ = 5.0 Hz, aryl-*H*, 2H). NOE was observed between the hydride at −45 ppm and the proton at 7.52 ppm. **9b**: −42 (br s, *H*-Ir, 1H), 7.3 (m, aryl-*H*, 1H), 7.33 (m, aryl-*H*, 1H), 7.35 (m, aryl-*H*, 1H), 7.56 (m, aryl-*H*, 1H), 7.58 (d, $^3J_{HH}$ = 6.6 Hz, 2H *H*-PNP-aryl), 7.92 (t, $^3J_{HH}$ = 6.6 Hz, lH, *H*-PNP-aryl). NOE was observed between the hydride at −42 ppm and the proton at 7.56 ppm. **9b**,**9c**: 51−51.5 (m, *P*-Ir-*P*). Anal. Calcd for **9**, $C_{29}H_{48}P_3F_6NBrIIr$: C, 39.15; H, 5.44. Found: C, 39.09; H, 5.39.

Reaction of [Ir(PNP)(COE)][PF_6] (1) with Anisole. Formation of [Ir(PNP)(H)(*o*-C_7H_8O)][PF_6] (10). A solution (1 mL) of [Ir(PNP)(COE)][PF_6] (**1**) (15 mg, 0.039 mmol) in anisole was heated at 60 °C for 3 h. The solvent was evaporated, and the resulting orange solid was washed consecutively with pentane and ether, resulting in complex **10** in almost quantitative yield. Complexes resulting from *meta*- and *para*-activated anisole were observed in trace amounts. ^{31}P{^{1}H} NMR (hydride coupled, CD_2Cl_2): 56.60 (d, $^2J_{PH}$ = 13.0 Hz). ^{1}H NMR (CD_2Cl_2) −42.00 (t, $^2J_{HP}$ = 13.0 Hz *H*-Ir-P), 1.2 (m, 36H, P-C(C*H*$_3$)$_3$), 3.55 (s, C*H*$_3$O; 3H), 3.7−4.0 (m, 4H, C*H*$_2$P), 6.4 (br d, $^3J_{HH}$ = 7.7 Hz, aryl-*H*), 6.7 (br t, J_{HH} = 6.8 Hz, aryl-*H*), 7.25 (d, $^3J_{HH}$ = 6.8 Hz, aryl-*H*), 7.6 (br t, $^3J_{HH}$ = 7.7 Hz, aryl-*H*), 7.65 (d, $^3J_{HH}$ = 7.7 Hz, 2H, *H*-PNP-aryl), 7.92 (t, $^3J_{HH}$ = 7.7 Hz, 1H, *H*-PNP-aryl). ^{13}C{^{1}H} NMR (CD_2Cl_2): 27.8−29.9 (m, P-C(*C*H$_3$)$_3$), 35 (m, *C*H$_2$P), 60 (m, *C*H$_3$OPh), 122.0 (m, PNP-aryl C3,5), 125.2−135.6 (singlets, phenyl carbons), 138.5 (s, PNP-aryl, C4), 138 (br t, C_{ipso}), 162.0 (s, PNP-aryl, C2,6). Anal. Calcd for $C_{30}H_{51}P_3F_6NOIr$: C, 42.85; H, 6.11. Found: C, 43.06; H, 6.03.

Lack of Reaction of [Ir(PNP)(H)(C_6H_4Cl)][PF_6] (8a) with an Anisole/Chlorobenzene mixture (1:1). A solution (1 mL) of [Ir-

(PNP)(H)(C_6H_4Cl)][PF_6] (**8a**) in anisole and chlorobenzene (1:1 molar ratio) was heated at 55 °C for 24 h. The resulting pale orange-like solid was washed consecutively with pentane and ether, resulting in complex **8a**, the starting complex. $^{31}P\{^1H\}$ NMR, ^1H NMR: vide supra.

Lack of Reaction of [Ir(PNP)(H)(*o*-C_7H_8O)][PF_6] (10) with a Mixture of Anisole/Chlorobenzene (1:1). A solution (1 mL) of [Ir(PNP)(H)(*o*-C_7H_8O)][PF_6] (**10**) in anisole and chlorobenzene (1:1 molar ratio) was heated at 55 °C for 24 h. The resulting orange solid was washed consecutively with pentane and ether, resulting in complex **10**, the starting complex. $^{31}P\{^1H\}$ NMR, ^1H NMR: vide supra.

Reaction of [Ir(PNP)(COE)][PF_6] (1) with a Mixture of Anisole/Chlorobenzene/Bromobenzene (1:1:1). (a) A solution (1 mL) of [Ir(PNP)(COE)][PF_6] (**1**) in anisole, bromobenzene, and chlorobenzene in 1:1:1 molar ratio was heated at 55 °C for 24 h, and the solvent was evaporated. ^{31}P NMR of the residue revealed three signals, which correspond to the *ortho*-activated anisole **10a**, *ortho*-activated chlorobenzene **8a**, and *ortho*-activated bromobenzene **9a** (vide supra) in a ratio of 35%, 32%, and 33%, respectively. ^1H NMR revealed three hydride signals, which corresponded to the three different complexes in a ratio similar to that shown by ^{31}P NMR. The hydrides were allowed to reach full relaxation (D1 = 45 s). $^{31}P\{^1H\}$ NMR, ^1H NMR: vide supra.

(b) A solution (1 mL) of [Ir(PNP)(COE)][PF_6] (**1**) in anisole, bromobenzene, and chlorobenzene in 1:1:1 molar ratio was heated at 70 °C for 48 h, and the solvent was evaporated. ^{31}P NMR of the residue revealed four signals, which correspond to the *ortho*-activated anisole **10a**, the *meta*- and *para*-isomers of activated chlorobenzene, bromobenzene, **8b**,**c**, **9b**,**c**, and anisole **10b**,**c** as well as *ortho*-activated chlorobenzene **8a** and *ortho*-activated bromobenzene **9a** (vide supra) in a ratio of 42%, 15%, 26%, and 17%, respectively. ^1H NMR revealed four hydridic signals, which corresponded to the four different complexes at a ratio similar to that shown by ^{31}P NMR. The hydrides were allowed to reach full relaxation (D1 = 45 s).

Acknowledgment. This work was supported by the Israel Science Foundation, Jerusalem, Israel, by the German Federal Ministry of Education and Research (BMBF) within the framework of German-Israeli cooperation (DIP), by the Minerva Foundation, Munich Germany, by the Lise Meitner-Minerva Center for Computational Quantum Chemistry, and by the Helen and Martin Kimmel Center for Molecular Design. D.M. is the Israel Matz Professor of Organic Chemistry, and J.M.L.M. is the Baroness Thatcher Professor of Chemistry.

Supporting Information Available: CIF files containing X-ray crystallographic data for complexes **1**, **6**, and **10a**. *XYZ* coordinates of all the computed complexes. This material is available free of charge via the Internet at http://pubs.acs.org.

OM060078+